

Copyright Warning & Restrictions

The copyright law of the United States (Title 17, United States Code) governs the making of photocopies or other reproductions of copyrighted material.

Under certain conditions specified in the law, libraries and archives are authorized to furnish a photocopy or other reproduction. One of these specified conditions is that the photocopy or reproduction is not to be “used for any purpose other than private study, scholarship, or research.” If a user makes a request for, or later uses, a photocopy or reproduction for purposes in excess of “fair use” that user may be liable for copyright infringement,

This institution reserves the right to refuse to accept a copying order if, in its judgment, fulfillment of the order would involve violation of copyright law.

Please Note: The author retains the copyright while the New Jersey Institute of Technology reserves the right to distribute this thesis or dissertation

Printing note: If you do not wish to print this page, then select “Pages from: first page # to: last page #” on the print dialog screen

The Van Houten library has removed some of the personal information and all signatures from the approval page and biographical sketches of theses and dissertations in order to protect the identity of NJIT graduates and faculty.

Abstract

Title of Thesis: Molecular modeling in anatoxin and other semirigid agonists.

Wen-chung Shang, Master of Science, 1989

Thesis directed by: Dr. Tamara Gund

Conformational search and molecular mechanics calculations were combined to investigate the structural flexibility of isoquinolone, the anatoxin series, and the ferruginine series. Ring searching allow all rational conformations to be generated.

Isoquinolone shows conformational similarity to isoarecolone but is much less potent which suggests that the proximity of the methyl group beta to the carbonyl groups affects the bioactivity of isoquinolone. The very active agonist-anatoxin, without a similar conformation as isoarecolone, shared a similar electrostatic potential contour in the vicinity *between* the two atoms connected to the electro-positive nitrogen and hydrogen bonding site. These phenomena were not found in ferruginine which has a similar conformation to anatoxin but less potent. The comparison of the various series implied that the geometric position of the nitrogen is not essential, but that the electrostatic potential around the binding sites is important.

Two FORTRAN programs were implemented and adapted to aid the molecular modeling. FDRING made an improvement in the speed of ring perception. CAGEATOM suggests a faster method to represent the electrostatic potential distribution on van der Waals surface.

MOLECULAR MODELING IN ANATOXIN AND
OTHER SEMIRIGID AGONISTS

By

Wen-chung Shang

THESIS SUBMITTED TO THE FACULTY OF THE GRADUATE SCHOOL OF
THE NEW JERSEY INSTITUTE OF TECHNOLOGY
IN PARTIAL FULFILLMENT OF THE REQUIREMENT FOR THE DEGREE OF
MASTER OF SCIENCE IN ENGINEERING SCIENCE

1989

Blank Page

APPROVAL

Title of Thesis: Molecular modeling in anatoxin and other semirigid agonists.

Name of Candidate: Wen-chung Shang

Thesis and Abstract Approved: _____

12/7/88

Dr. Tamara Gund

Date

Department of Engineering Science

Signatures of other members

of the thesis committee:

12-1-88

Date

12/7/88

Date

Vita

Name: Wen-chung Shang

Present address:

Permanent address:

Degree and date to be conferred: Master of Science, 1989

Date of birth:

Place of birth:

Secondary education: Kaohsiung High School, 1977

Collegiate institutions	Date	Degree	Date of Degree attended
Tung-Hai University	1980-1984	B.S.	Jun., 1984
New Jersey Institute of Technology	1986-1988	M.S.	May., 1989

Major: Engineering Science

Position Held: Graduate Assistant, Jan., 1987 - May., 1987

Research Assistant, Sept., 1987 - Sep., 1988

Department of Chemistry/Chemical Engineering

New Jersey Institute of Technology

Newark, NJ 07104

To my parents.

Acknowledgements

I particularly wish to express my appreciation and gratitude to Dr. T. Gund for her guidance, insight and for the kindness she show me during my days in N.J.I.T. I also wish to acknowledge Dr. A. Greenberg and Dr. D. Kristol for careful reading of the thesis. But the greatest and most crucial help has come from my wife. She has been the rock on which I have always relied for encouragement and inspiration.

Table of Contents

Chapter	Page
Acknowledgements	ii
List of Tables	v
List of Figures	vi
I. Introduction	1
A. Agonist and Antagonist	1
B. Acetylcholine	1
C. Computer Molecular Modeling in Chemistry	4
D. Goal of Present Research	5
II. Methodology	6
A. Ring Perception	6
B. Conformation Search	8
C. Molecular Mechanics	10
D. Structural Superposition	12
E. Atomic Point Charges	13
F. Molecular Electrostatic Potential	14
G. Cage Atoms	15
III. Results and Discussion	17
A. Ring Perception	17
B. Isoquinolone	18
C. Anatoxin	19

D. Ferruginine	21
E. Cage Atoms	23
IV. Conclusion	24
V. Tables	26
VI. Figures	43
VII. Appendix	71
VIII. Reference	79

List of Tables

Table		Page
1.	List of rings of Tubocurarine	26
2.	Coordinate of FERC	27
3.	Coordinate of FERF	28
4.	Coordinate of FERH	29
5.	Coordinate of FERN	30
6.	Coordinate of ANAH	31
7.	Coordinate of ANAN	32
8.	Coordinate of ANAC	33
9.	Coordinate of ANAF	34
10.	Coordinate of MET1Z	35
11.	Coordinate of MET4Z	36
12.	Coordinate of MET5Z	37
13.	Coordinate of MET6Z	38
14.	ESP distribution on surface of ferruginine, anatoxin, isoquinolone . .	39
15.	Energy and Beers distance profile of FERN	40
16.	Energy and Beers distance profile of ANAZ16	40
17.	Energy and Beers distance profile of ANAZ84	41
18.	Energy and Beers distance profile of ANAZ175	41
19.	Energy and Beers distance profile of ANAZ510	42

List of Figures

Figure	Page
1. Structure of anatoxin, ferruginine, and isoquinolone	43
2. Structure of tubocurarine	44
3. Energy vs dihedral angle for anatoxin series	45
4. Distance from nitrogen to the van der Waals surface of oxygen vs di- hedral angle for anatoxin series	46
5. Energy vs dihedral angle for ferruginine series	47
6. Distance from nitrogen to the van der Waals surface of oxygen vs di- hedral angle for ferruginine series	48
7. Color coded ESP on van der Waals surface of isoarecolone	49
8. Color coded ESP on van der Waals surface of ANAH	50
9. Color coded ESP on van der Waals surface of ANAC	51
10. Color coded ESP on van der Waals surface of ANAF	52
11. Color coded ESP on van der Waals surface of ANAN	53
12. Color coded ESP on van der Waals surface of FERH	54
13. Color coded ESP on van der Waals surface of FERC	55
14. Color coded ESP on van der Waals surface of FERF	56
15. Color coded ESP on van der Waals surface of FERN	57
16. Color coded ESP on van der Waals surface of MET5Z	58
17a. Fitting on N C O in ferruginine series	59
17b. Fitting on N C O of ferruginine series with isoarecolone	59
18a. Fitting on N C O in anatoxin series	60
18b. Fitting on N C O of anatoxin series with isoarecolone	60

19a. Fitting on N C O of isoquinolone MET1, MET4, MET5, MET6 with isoarecolone	61
19b. Fitting on N C O of isoquinolone MET1Z, MET4Z, MET5Z, MET6Z with isoarecolone	61
20. Fitting on O=C-C=C of anatoxin and ferruginine with isoarecolone .	62
21. Electro static potential using CAGECON method of isoarecolone . . .	62
22. Contouring at 150 kcal/mole of the ESP of isoarecolone	63
23. Contouring at 150 kcal/mole of the ESP of ANAH	64
24. Contouring at 150 kcal/mole of the ESP of FERH	65
25. Contouring at 150 kcal/mole of the ESP of MET5Z	66
26. Contouring at 30 kcal/mole of the difference of ESP when anatoxin fit isoarecolone at N C O	67
27. Contouring at 30 kcal/mole of the difference of ESP when anatoxin fit isoarecolone at C=C-C=C	68
28. Contouring at 30 kcal/mole of the difference of ESP when ferruginine fit isoarecolone at N C O	69
29. Contouring at 30 kcal/mole of the difference of ESP when ferruginine fit isoarecolone at C=C-C=C	70

Chapter I

Introduction

A. Agonist and Antagonist

Biological control and the response systems of humans are controlled by the nervous system. Nerve cells are not infinitely long, but have discrete length. It is chemical reactions which connect nerve cells and nerves with muscles. The chemicals involved in such biological processes are called *neuro-transmitters*, and the mode of action of these chemicals are of great interest to pharmacology.

Some synthetic molecules will produce a similar effect to natural compounds when injected. Such molecules, along with the naturally occurring molecules are referred to as **agonists**. Molecules which bind to the same receptor (active site where the small molecules and a macro molecule interact) in such a way that the receptor is blocked and the natural transmitter is rendered inactive are called **antagonists**.

The ability to predict the interaction of the macromolecular receptors and their small ligands (agonists/antagonists) leads to the possibility of designing new compounds, which could prove useful as research tools or novel drugs.

B. Acetylcholine

Acetylcholine was one of the first nerve transmitters identified at the beginning of this century. The acetylcholine receptors which bind to the basic neurotransmitter are representative of a class of membrane proteins responsible for the electrical activity of the nervous system. The receptor while binding to an agonist responds by opening a channel allowing ions to pass through the membrane. The ion flows produce electrical

signals which cause nerve impulse activity, such as muscle contraction.

Two basic types of receptors for acetylcholine are known, 'muscarinic' and 'nicotinic'. Muscarinic receptors are found at parasympathetic neuroeffector junctions and nicotinic receptors at skeletal neuromuscular junctions and autonomic ganglia.

The mechanism by which an agonist combines with the acetylcholine receptor to initiate changes in conformation that result in the opening of the ion channel is still unknown. The agonist is believed to remain bound to the receptor during activation which suggests that the acetylcholine receptor molds its conformation to fit the agonist structure. Since the actual structure of the receptor is unknown, indirect methods have been used to gain insight into the structure, the binding mechanism, the geometry of the receptor site, and the bound conformations of agonists and antagonists. One method of studying the binding process is by structure-activity relationships. This is, however, difficult because most agonists are flexible molecules and their bioactive conformations are undetermined. Rigid agonists solve this problem since the number of possible conformations is greatly diminished. The number of possible complementary conformations of the receptor are likewise reduced.

The conformations of acetylcholine and other cholinergic ligands have been studied experimentally and computationally by many workers. Most of the calculations involved flexible molecules, and centered around deriving energy surfaces of fixed conformations with varying torsional angles of interest. For example, two receptor models for nicotinic and muscarinic binding were proposed. One by Kier[2] is based upon comparisons of interatomic distances separating atomic centers of functional importance. The other, by Chothia and Pauling[5] is based on preferred values of relevant dihedral angles from x-ray crystallographic studies of potent cholinomimetics. Both models are based on fixed conformations of agonists and antagonists bound to the receptors, and both fail to explain the activity of the reverse ester of acetylcholine.

DonelSmith[3] found it necessary to invoke a model based on flexible receptors and ligands.

In 1970 Beer's and Reich[4] proposed a pharmacophoric distance for active nicotinic agonists. They predicted that the optimal distance between the site of coulombic interaction(quaternary nitrogen) and hydrogen bonding interaction(ester oxygen) for a nicotinic agonist is 5.9Å. Pullman, Courriere and Coubeils[8] performed quantum mechanical studies (PCILO) on acetylcholine, nicotine and muscarine to determine their conformational and electronic properties. Their conformational studies agreed with experimental data and their electronic studies revealed that the nitrogen on acetylcholine is almost neutral and the positive charges are spread over the three methyl groups, thus forming a large positive area for coulombic interaction with the receptor. Pauling[5] performed calculations on a series of anticholinergic substances, and discovered a consistent low energy conformation in all but two compounds, and determined which functional groups were necessary for pharmacological activity. The calculated energy of the consistent conformation was generally less than the crystal conformations, and for the two remaining structures the consistent conformations were only 2 kcal higher than the crystal structures. Weinstein[6] performed quantum mechanical calculations on 3-acetoxyquinuclidine and found that the molecule could adopt the gauche acetylcholine binding conformation. The interaction pharmacophore of the active species was defined by the electrostatic potential fields which were generated, and revealed a reactivity pattern identical with acetylcholine.

Activity and specificity varies with conformations and configurations of the molecule. Computer calculations can now accurately predict preferred conformations, charge densities, electrostatic potential contours and pharmacophoric patterns[7]. A systematic computer graphic study of semirigid receptor agonists and antagonists could assist in correlating the structures of these drugs to their actions. Semirigid

conformations can be obtained by the presence of rings within a structure which removes degrees of freedom and restricts the available geometries to a small subset of those available to its acyclic counterparts. This restriction may alter the chemical reactivity of functional groups within the molecule through changes in either the strain of the structure or the steric environment of the groups. Isoarecolone was used as a conformational template in this paper because it is one of the most potent agonists possessing some conformational rigidity.

C. Computer Molecular Modeling in Chemistry

Molecular modeling is a technique that allows calculations and visualization of some natural properties of molecules. A computer-based model may offer useful inferences about geometric, steric, and even chemical properties which are based on the fact that atoms in molecules prefer to orient themselves in well-defined ways. As the flexible and vibrating aspects of molecular structure may be represented by a mechanical model of balls connected by springs, the computer model may use restraining forces to represent the same aspects more quantitatively.

The discipline of molecular modeling is based on classical physics, which treated the universe as a collection of objects subject to the classical electrical, magnetic, and gravitational forces. Molecular modeling can be used to study reactivity, stereoselectivity of reactions, stereoisomerism, reaction mechanisms, or to derive models to explain and predict biological activities of drugs. It gives chemists a sense of the properties of a compound without having to hold a molecular model of the molecule at hand. With the facility of high speed, high resolution graphics terminals connected to a computer, manipulation of a whole or part of the structure, highlight a portion

of a molecule, coloring, and contouring can be performed easily. Software packages for molecular modeling, which are commercially available, can be used to search for correlations among molecules with common biological activity. For example Palmer and coworkers have used computer modeling to propose a model of the Acetylcholine receptor site[9].

D. Goal of Present Research

The malfunctioning of acetylcholine mediated transmission of nervous signals (which involves nicotinic and muscarinic receptors) is responsible for many diseases incurred by man[1]. We are interested in studying the nicotinic acetylcholine receptor. The work involves molecular modeling of nicotinic agonists to determine their structures and electrostatic properties and derive a model based on steric and electrostatic requirements for potency. The derivation of this model will facilitate the design of novel agonists.

Chapter II

Methodology

The facilities used in this study are an Evans and Sutherland PS330 color Vector graphics terminal connected to a VAX 11/785 mini computer. The HP-7445A plotter is used for plotting and the John von neuman Supercomputer CYBER 205 is used for extensive calculations.

A. Ring Perception

The ring restriction may alter the chemical reactivity of functional groups within the molecule through changes in either the strain of the structure or the steric environment of the groups. This feature can be used to restrain the flexibility of non-ring structures and may highlight the distinction of reactive functional groups. Thus fast ring perception by computer becomes a plausible starting step of generating possible ring structures. It may not be necessary to find all possible rings in a structure but the speed of the program discussed in this paper is fast enough so as to be practical.

Human recognition of rings from pictorial representation of graphs is rapid, but sometimes leads to incomplete results when trying to find all rings in a complex polycyclic graph. The computer by using an algorithm, can be directed toward the perception of rings [10-14]. Computers deal with graph representation through vertices and edges. The algorithm implemented in this paper first removes from the structure those atoms and bonds not involved in the ring. This is done by recursively pruning all atoms which have only one connection with all the other atoms until only the ring assemblies, and the atoms and bonds interconnecting them, are left.

The second step concerned a concept of homeomorphically reduced graph(HRG)[15].

The HRG is a subgraph of previous pruned graphs which has only the vertices(atoms) of degree three or more, called irreducible vertices. All bonds between two irreducible atoms are retained in HRG. Then matrix manipulation methods are used to enable one to consider many paths simultaneously. A fundamental set of rings(or basis set of rings), rings set containing the minimum number of rings which contain all ring atoms and bonds in the structure, are obtained first. After the basis rings set are located the rings of interest can be decided by taking the logical exclusive or (XOR) of the bonds of every combination of one to n of the n basis rings. The process of obtaining all possible rings by taking the XOR of the bond sets of the basis rings has been developed as an algorithm by Gibbs[16]. The speed of Gibbs' algorithm is highly dependent on the number of rings in the basis set, since the logical exclusive or is taken for all combinations of one to n basis rings. If combination of the basis rings in one assembly of rings with any combination of basis rings in the other assembly will not result in any rings, interassembly combination of basis rings is unnecessary. Therefore by detecting the assemblies of rings the speed of Gibb's algorithm is improved.

The Welch's and Gibbs' algorithms implemented here use binary sets and supersets to achieve significant improvements in memory requirements and execution times. A faster algorithm for ring perception method was discussed[17], but the logical set operations are not provided and is machine dependent, which depends on the maximum logical bits operation at one computer operating cycle. In VAX 11/785 it is 32 bits for a data type *longwords* and the corresponding logical bitmap operation can take two *longwords* at a time, so a group of set calculation subroutines are developed in VAX FORTRAN(see Appendix I). The size of a *longword* may limit the amount of atoms allowed in a structure, thus matrix is used to extend the limit. The dimension is defined as 4 in this paper which can operate on $4 \times 32 = 128$ atoms simultaneously, but can be modified to a greater amount easily. Without almost

any modification, both the Wipke's Welch-Assembly-Gibbs and HRG algorithms are rewritten in VAX FORTRAN. FORTRAN language was chosen for it is possible to vectorize the program to run it on a CYBER 205 supercomputer which supports only the FORTRAN and C compilers, since program portability became important in software development today.

B. Conformation Search

RCG5[21] is used to provide a systematic conformational search procedure. A molecule with some degree of torsional freedom is submitted to a conformational analysis based on the screening of the van der Waals contact distance. While the conformational space is being explored by breaking some rotatable bonds and increasing the torsion angle in definite steps the conformers in which short distance contacts exist are being eliminated. The evaluation of the interatomic distance contacts is decided according to the atomic van der Waals radii.

A conformation is rejected based on the following criterion: two atoms, separated by at least three bonds, cause the distance to be shorter than the sum of their respective van der Waals radii, which is impossible. A conformation search will be very time-consuming and can be directed and/or reduced by pharmacological properties. Ring constraints also make the searching faster than for acyclic conformations.

Each rotatable bond is defined by a chain of four connected atoms. The middle two atoms actually define the rotatable bond, while the first and fourth atoms are needed to measure the value of the torsion angle. For example dihedral angle of rotatable bond ABCD is defined as the angle of line C-D and the plane A-B-C.

The primary criterion for determining the validity of a conformation in RCG5 is the sum of the van der Waals radii of the atoms. This set of radii can be altered by an overall multiplication screening constant, a smaller number 'softening' the contact

and permitting more conformations to meet this criterion.

Some parameters of the RCG5 must be set before the ring atoms are submitted to RCG5. These parameters are the van der Waals screening factor, bond length variance, and angle variance. A larger parameter value is appropriate to have an overall look in the beginning, but an optimized value becomes critical because every possible conformation must be generated. The combinations of the database of molecular structures and conformation search allow us to have a systematic way to create rational starting conformations for minimizations later on.

Since ring conformations rarely differ by only torsional angles, the amounts of permissible variation in the length of the closure bond and the valence angles about that bond should be adjustable. Thus a bond length variance of 0.1 Å of the initial length, a bond angle variance of 5 degrees accepts conformations with bond angles differing by as much as 5 degrees from the original. The rotatable bonds chosen for Anatoxin are 11-5, 1-5, 1-2, 2-26, 3-26.(Figure 1-I) For each of the rotatable bonds an increment of 10 degrees in torsion angle is assigned to create the new conformations. The ring closure bond(3-26) range is set to be 0.5-2.5Å, two ring closure angles(26-3-10, 2-26-3) range from 90 to 130 degrees, and three ring closure torsion angles (1-2-26-3, 2-26-3-10, 26-3-10-11) ranges are set to 180 degrees. The van der Waals radii scaling factor is 0.7 to allow more conformations to be generated because of the semi-rigidity of Anatoxin. After the search, RCG5 generates 517 conformations which are sent into FILTER(program in association with RCG5) to delete duplicate conformations. The remaining 27 conformations are then minimized by MM2 and separated into 3 categories according to their N-O distances. The final comparison of these conformations are done by using SYBYL[23] on a PS330 by the "FIT" function, the conformations were found to lie in the same category and are almost the same. The three conformations found were named ANAZ175, ANAZ510, ANAZ84, ANAZ16.

Rotable bonds chosen for Ferruginine are 11-5, 1-5, 1-2, 2-3 (figure 1-II). The torsion angle increment, ring closure bond range, angle range, torsion angle range are set to be the same as Anatoxin. 54 conformations are generated by RCG5 by using the same procedures as above. Only one conformation remained after all the filter processes. This may be due to the fact that Ferruginine is more rigid than Anatoxin and less conformations are geometrically possible.

There are three rings in Isoquinolone: Ring 1:1-4-7-5-2-13-1 Ring 2:1-9-8-6-3-13-1; Ring 3: 1-9-8-6-3-13-2-5-7-4-1. The same criterion is applied and 4 unique conformations remained, named as MET1, MET4, MET5, MET6. Each of the four conformations has an enantiomer with the same coordinates except the sign of Z coordinate values are reversed. Finally there are eight conformations to be considered for Isoquinolone.

C. Molecular Mechanics

Molecular mechanics employs the fundamental formulations of vibrational spectroscopy. It is assumed that bonds have "natural" lengths and angles and molecules will adjust their geometries so as to take up these values. In addition, nonbonded atom interactions are included using van der Waals potential functions. Molecular mechanics calculations require a force field, that is, a relationship between the energy of a molecular species and its internal coordinates. A force field contains adjustable parameters that are optimized to obtain the best fit of calculated and experimental properties of the molecules, and it is assumed that corresponding parameters and force constants may be transferred from one molecule to another. In general a molecular mechanics force field includes bond stretching, angle bending, torsion, and van

der Waals interactions.

$$V = \sum V_{stretch} + \sum V_{bend} + \sum V_{torsion} + \sum V_{VDW}$$

More elaborate force fields may also include either 1,3-nonbonded interactions, or cross-interaction terms, electrostatic terms, and so on.

The MM2 program was used to perform the conformational analysis of molecules in this paper. The Allinger force field treats small molecules well.

$$E = + \sum_{bonds} K_r (r - r_{eq})^2 \quad (\text{II.1})$$

$$+ \sum_{angles} K_\theta (\theta - \theta_{eq})^2 \quad (\text{II.2})$$

$$+ \sum_{dihedrals} V_n [1 + \cos(n\phi - \gamma_n)] / 2 \quad (\text{II.3})$$

$$+ \sum_{i < j} [A_{ij} / R_{ij}^{12} - B_{ij} / R_{ij}^6 + q_i q_j / (\epsilon R_{ij})] \quad (\text{II.4})$$

$$+ \sum_{H-bonds} [C_{ij} / R_{ij}^{12} - D_{ij} / R_{ij}^{10}] . \quad (\text{II.5})$$

the first three terms represent the mechanical energy. The remaining terms represent non-bonded van der Waals, electrostatic, and hydrogen bonding respectively. The symbols used are r to represent the bond length, θ the bond angle, ϕ the dihedral angle, R_{ij} the distance between any two atoms i and j , q_i the charge on atom i , and ϵ , the dielectric constant. ϵ is generally chosen as 1.0, but can be made distance dependent ($\epsilon \propto R_{ij}$) in order to simulate the effect of the solvent medium. The distance dependent dielectric damps the effect of the long range interactions, thus increasing the effect of short range interactions and simulating the effect of solvent polarization.

The force field parameters are r_{eq} (the equilibrium bond length), K_r (the bond stretching constant), θ_{eq} (the equilibrium bond angle), K_θ (bond angle bending constant), γ_n (the torsional angle phase factor), V_n (the torsional angle constant), A_{ij} and B_{ij} (the nonbonded parameters), and C_{ij} and D_{ij} (the hydrogen bond parameter).

Conformation energy minimizations are done using a revised version of Allinger's MM2 program, modified by T. Halgren to handle formally charged molecules and parametrized for ammonium salts in collaboration with J. Snyder.

Only MM2 parameters were considered in this paper as, MM2 minimized geometries were found to be identical to those found from semi-empirical methods (CNDO/2, MNDO etc.) for several of the model compound.

D. Structural Superposition

Among various methods developed in computer-aided molecular modeling, molecular superposition methods are widely used for structural data investigation. The essential purpose is a pairwise comparison of molecules, one molecule acting as a reference, the other being used for comparison, in order to discover structural and geometric similarities or differences. This is achieved by geometric least-squares minimization on the three-dimensional atomic coordinates.

Molecules were superimposed, displayed and manipulated using the SYBYL program. The comparison was made by superimposing one structure upon the other using the RMS(Root Mean Square) fitting function of SYBYL. In this procedure, a set of selected atoms of one molecule are superimposed on a set of selected atoms in a second molecule by a least-squares fitting algorithm. These algorithms will reorient the second molecule to make the summation of the distance of designated atoms of two molecules as small as possible. During the reorientation the bond lengths, angles or torsion angles in any of the molecules did not vary. The resulting RMS values show the quality of the fit. Differences in atomic positions in the superimposed structures highlight the regions of significant conformational change.

Computer superposition of the molecules in this paper are performed to examine the closeness of fit at coulombic and hydrogen bonding sites. The weights of the

superpositions are assigned to 1 for each chosen position because they are equivalent in pharmacophore constituents.

E. Atomic Point Charges

The information of the distribution of electrons can tell the fact that the chemistry, the affinity, the efficiency and reactivity of a molecule are properties of electrons. When molecules encounter it is the electrons which interact. Thus approximate charge distributions are helpful to gain the inner view of reaction characteristics.

It is artificial to assign partial charges to atoms. In reality the charge is a smooth function of nuclei surrounded by electrons, and for reasonably small molecules the electrostatic field can be calculated. If a quantitative comparison is necessary, the method of calculating the electron density in a defined sphere

$$Q(R) = \int \int \int \Psi^* \Psi_r^2 \sin \theta dr d\theta d\phi$$

where Q is the charge of radius R , Ψ is the molecule wave function. In the above equation a molecular wave function is squared and summed over a sphere for which the radius and location are specified.

Another alternative way is to place the calculated electrons in the orbital, and summed the electrons within a range of an atom, then subtracted from the nuclear charge. Methods such as Mullikan population analysis split the electrons in localized bonds between two atoms participating in the bond; CNDO uses parameters to give partial charges; Allinger uses bond dipoles, summing contributions on individual atoms.

An incoming reagent senses an overall electrostatic field, not the charge on individual atoms. Various methods can give us different charge distributions but the overall contour look of the electrostatic field is of more realistic and practical use

than finding the exact atom charge. Partial charges were calculated using Dewar’s MNDO program from MOPAC in this paper. No geometry optimization is performed during the calculation. MOPAC point charges provide similar electrostatic potentials as obtained from *ab initio* methods.

F. Molecular Electrostatic Potential

The electrostatic molecular potential is taken as the interaction energy between a unit positive charge and the unperturbed molecular charge distribution. The full calculation of an ‘exact’ potentials is

$$V(k) = - \int \rho(l) \frac{1}{r_{lk}} dv_1 + \sum_{\alpha} \frac{Z_{\alpha}}{R_{\alpha k}}$$

where Z_{α} is the nuclear charge of nucleus α , $\rho(l)$ is the electron density.

However, approximations are used more frequently. Once partial charges have been assigned, electrostatic potential can be calculated. The electrostatic potential(ESP) energy are calculated and contoured on the van der Waals surface by ARCHEM. The atomic point charges are used in Coulomb’s law

$$V = 332.0 \sum \frac{q_i}{\epsilon |r_i - F|}$$

to compute the energy V felt by a point charge at position F being influenced by a system of charges q_i at positions r_i . The dielectric constant ϵ is set to unity. The constant 332.0 converts the resulting energy value to Kcal/mol. The points are calculated so that they are distributed on the van der Waals surface uniformly. The atomic radii determine the extent of this surface. The area of ESP are determined by counting points within a range and multiplying by the area per point, since the area per point are slightly different for each atom type. The areas are very dependent on the atomic radii, which are as follows (\AA) C, $sp_3=1.70$; C, $sp_2=1.74$; O=1.50; N=1.60;

H=1.30; H, hydroxyl=1.00. Electrostatic potentials were calculated in reference to an incoming positive charge, and since the molecules have net positive charge, are calculated as repulsive energies.

The electrostatic map gives a view of the initial interaction of the molecule with a reagent; as the reaction proceeds, electron transfer occurs and the electrostatic picture is altered. Thus this picture gives us only an initial state, the subsequent electrostatic potential will no longer be the same.

G. Cage Atoms

The electrostatic potential distributed on the van der Waals surface of a molecule can be calculated by the cage function in ChemX[24]. Command "CALCULATE CAGE" will position dummy atoms (atom type A) over the van der Waals surface of the structures included in the display.

A grid is first constructed around the structure with the axes of the grid aligned with the x, y and z axes of the structure and then step through the grid points just created. Dummy atoms are initially positioned at all grid points that lie just outside the structure, and are connected to any adjacent atoms that lie within one grid step along each axis within the grid (ie. to the nearest neighbors). Thus at the first attempt any dummy atom may be connected to up to six other atoms. The algorithm generates connections between the atom and all other dummy atoms that are less than three grid steps away where no more than one step can be made along any axes for any atom that has less than four connections. This generates a cage of dummy atoms which are contracted onto the surface of the structure, with the direction of motion for each atom being in the direction of the initial scan. The radius of the dummy atom is set to zero when a van der Waals surface is being used.

The "/MESH" qualifier allows one to change the grid step size used when set-

ting up the grid and scanning the structure. It is set to 1.0 Å by default, and is set to 0.5 Å for more dummy atoms to be generated on the surface. “/NOCONNECTIONS” qualifier prevents Chem-X from calculating the approximate surface area of the structure and allows the calculation to take less time.

After the dummy atoms are generated the structure will contain all the coordinates of the dummy atoms. The electrostatic potential of each dummy atom is then calculated by “CAGECONT” which will assign a dummy atom type ($A_1 \dots A_n$) according to the desired range the electrostatic potential of dummy atoms are in. This new structure is then read back into the Chem-X program and the “SET ATOM” command is executed to assign different colors to different electrostatic potential ranges. After all these procedures the structure can be displayed with dummy atoms of different colors showing the electrostatic potential range.

The “CAGECON” program takes advantage of the “CAGE” function of Chem-X and gives the electrostatic potential on the van der Waals surface just like ARCHEM but at a much lower speed (1/100th of ARCHEM). If greater accuracy must be achieved the “CONNOLLY SURFACE” function can be used to improve the distribution of dummy atoms but more computer time will be used in the process.

Chapter III

Results and Discussion

The symbols used in the following discussion are FER for ferruginine, ANA for anatoxin, and MET, METZ—two enantiomers of isoquinolone. Numbers following the symbols are the numbering from RCG5. The last letter of ANA and FER represents four possible ways of attachments of methyl group(s) to the nitrogen, C representing one methyl group attached to the nitrogen which is closer to the oxygen than the F. The H is two hydrogens and N is two methyl groups attached to nitrogen respectively. Beers-Reich distance is the distance between the nitrogen and the van der Waals extension of the oxygen. The corresponding colors of energy ranges are 0–40 purple, 40–60 dark blue, 60–80 blue, 80–100 green, 100–120 orange, 120–140 brown, 140–160 red.

A. Ring perception

Set operation subroutines are implemented and combined with Welch-Assembly-Gibbs and HRG algorithms successfully. The speed of the program FDRING(Appendix) was compared with the previous program “CYCLE” and found to be 5 times faster in CPU time when the sample structure submitted was tubocurarine. The accounting message from the VAX/VMS is as follows (CPU time in seconds)

	CYCLE	FDRING
Charged CPU time	76.06	15.23

There are 72 possible rings(cycles) in tubocurarine (Table 1,Figure 2), and three in anatoxin, ferruginine and Isoquinolone. Although this program is of no great con-

tribution in modeling small molecules, it will become useful in modeling of proteins, and other macromolecules.

B. Isoquinolone

Isoquinolone is a semirigid, nicotinic agonist. The disposition of this agonist's nitrogen and carbonyl group conforms well to a prevailing notion of a pharmacophore for the nicotinic receptor. The eight conformations of isoquinolone from RCG5 were minimized by MM2. Coordinates of each optimized conformation are presented in Table 10-13 (the coordinates of MET1, MET4, MET5, MET6 are omitted because their z-coordinates are the inverse sign of MET1, MET4, MET5, MET6 respectively). The results of energy and Beers-Reich distance are shown:

	Final energy	Beers distance	dihedral angle O=C-C-C
MET1	27.38	6.34	-7.44
MET1Z	27.38	6.34	7.44
MET4	26.94	5.78	8.51
MET4Z	26.94	5.78	-8.51
MET5	18.44	6.19	-1.97
MET5Z	18.44	6.19	1.97
MET6	28.83	6.28	-1.55
NET6Z	28.83	6.28	1.49

(O=C-C-C represent the dihedral angle of the ketone and the ring.)

From the above table we can see that enantiomeric conformations have the same energy, Beers-Reich distance, and O=C-C=C angle which agrees with the theory that enantiomers have the same physical properties. The Beers-Reich distance of MET4 is

too short to be a possible bioactive conformation. The eight conformations are then fitted on isoarecolone (figure 19a, 19b). From the superpositions we see that MET5Z fits on the template isoarecolone better than the other derived conformations from Table 10–13. MET5Z fits both the ring and the dimethyl groups of isoarecolone. From this result we could predict that isoquinolone should be a potent drug. But on the contrary isoquinolone is only 0.0003 as potent as isoarecolone (defined as unity). The energy difference between MET5Z and the other conformers (MET1Z, MET4Z, and MET6Z) is 8–9 kcal. MET5Z, which fits best on the template is also of the lowest energy and would be expected to predominate. The two rings in isoquinolone show some flexibility but were constrained to one conformation due to this energy barrier. Another interesting result is that the fitting of the enantiomer of MET5Z–MET5 did not fit well onto isoarecolone. The population of either conformation is not known, but if both enantiomers are present then the overall potency could be lower due to the presence of MET5.

The color coded electrostatic potential of MET5Z is presented in figure 16. The corresponding area of each range is shown in table 14. From figure 16 we can see that the electrostatic potentials around the cationic heads (around nitrogen) of MET5Z are similar in shape to that found in isoarecolone and that the vicinities of the carbonyl bond acceptors are also similar. This similarity would also predict an active agonist but isoquinolone was found to be a very weak agonist. One possible explanation for the inactiveness of isoquinolone as an agonist is that MET5Z contains a steric obstruction in the acetyl methyl region which may prevent binding. This can be seen in figure 16, where the methylene group beta to the carbonyl intrudes on that space.

C. Anatoxin

Anatoxin like isoarecolone is a very potent agonist. Four anatoxin conformations remained after the ring searching from RCG5, ANAZ16(minimized energy 1 kcal/mol), ANAZ84(minimized energy 43.85 kcal/mol), ANAZ175 (minimized energy 9.00 kcal/mol), ANA510Z (minimized energy 10.66 kcal/mol). The optimized energy of ANAZ84 is too high compared to other derived conformations. Therefore it is eliminated as a possible bioactive conformation. Although ANAZ16 is of lowest energy, it is eliminated as a possible bioactive conformer because the dihedral driver calculation shows the s-cis to be an inaccessible conformer(ΔE s-cis/s-trans = 46 kcal/mol).

The energy profile and Beers-Reich distance of ANAZ175 and ANAZ510 are very similar(figure 3,4. table 18,19). ANAZ175 has a boat like shape and ANAZ510 has a chair like shape in the seven member ring. Conformational studies implied that anatoxin can flip easily between the two conformations ANAZ175 and ANAZ510($\Delta E=1-1.5$ kcal/mol). The difference between the energy profile and the Beers-Reich distance profiles in ANAZ510 and ANAZ175 are small, except that ANAZ510 shows only one minimum and ANAZ175 has two minimum conformations around 180 and 330 degrees. Also, the Beers-Reich distance of ANAZ175 at 330 degrees is larger than 6 angstroms and the distance in ANAZ510 is about 5.7 angstroms. ANAZ175 is preferred over ANAZ510 as the candidate for the bioactive conformation, but ANAZ510 still needs to be considered. By using the function "SKETCH" in SYBYL, a series of anatoxin structures are generated ANAF, ANAH, ANAC corresponding to the ways that the methyl group is attached to the nitrogen.

The fitting on the NCO within the anatoxin series are shown in figure 18a. From the figure we can see that the anatoxin series is more flexible compared to the ferruginine series. The ring conformations of ferruginine do not change with N-Methyl

substitution while N-Methyl substitution in anatoxin produces larger changes in conformations of the ring. The anatoxin series were superimposed on isoarecolone in different ways (figure 18b). When the Beers-Reich superposition criteria was employed, the fit was not good. However, fitting on the O=C-C=C(hydrogen bonding site) produced a good fit at the acetyl group but not at the nitrogen(Figure 20). The Beers-Reich distance in anatoxin is satisfied but is not a sufficient criteria for agonist potency. If we compare the electrostatic potential contour with isoarecolone(figure 22,23) , the shape of the electrostatic potential of the hydrogens attached to nitrogen in anatoxin looks similar to the shape of the axial methyl group attached to nitrogen of isoarecolone. The phenomenon that charges on nitrogen are distributed to the two attached groups are observed for many potent agonists. One possible explanation could be that once the structure satisfies the Beers-Reich distance the electrostatic potential distribution on the axial attached group is more important than on the equatorial. It is also implied that the fitting of nitrogen is not essential, but rather the electrostatic potential it created around itself in the direction of the axial substituent. Also, if we examine the contouring of energy the difference(30 kcal/mol) between anatoxin and isoarecolone according to the two fitting methods(figure 26), we can see that the fit at the O=C-C=C site generates two electrostatic potential differences which are in the area of the side ring of the anatoxin and the equatorial methyl group. If the fitting is at N C O then there is an extra potential difference around the O=C-C=C which is not seen in previous fitting methods. The preceding result suggests that even if we fit on the O=C-C=C the positive electrostatic potential around the nitrogen of anatoxin remained which implied that the position of the nitrogen is not very essential but the way that the charge is distributed to the surrounding atoms.

D. Ferruginine

Ferruginine has a similar conformation as anatoxin but is less potent. From the ring search we had only one conformation that remained—FERH(table 4). This is due to the rigidity of ferruginine that constrains the flexibility of the ring structure. Using the same procedures as in the anatoxin series, a series of ferruginine structures were generated from this molecule FERF, FERC, FERN corresponding to the ways of attaching a methyl group on the nitrogen(Table 2–5). Minimized energies of these four structures are FERN (17.27 kcal/mol), FERC(10.06 kcal/mol), FERF(10.64 kcal/mol), FERH (6.92 kcal/mole). The four conformations showed similar energy and geometry profiles. Dihedral angle calculations were performed(figure 5,6), and show that the energy profiles of each structure are almost the same, which suggests that the addition of methyl groups to the nitrogen has little effect to the conformation of ferruginine. The ferruginine series fits well on each other and are shown in figure 16a. Both of the preceding observations again prove that ferruginine has a very rigid conformation. However, none of the conformers showed a good fit with isoarecolone or anatoxin at NCO. The fitting at the hydrogen bonding site($O=C-C=C$) with isoarecolone (figure 20) resulted in a similar situation as anatoxin, except that the nitrogens are further apart than in anatoxin. This could be the reason why ferruginine is less potent than anatoxin.

Furthermore, the electrostatic potential on the van der Waals surface of ferruginine is calculated and plotted by ARCHEM(figure 12, table 14). From the pictures we see that the pattern of color distribution of ferruginine is similar to isoarecolone which suggests that ferruginine should be potent. One possible explanation for ferruginine being less potent than anatoxin is that the relative position of the most positive electrostatic potential to the carbonyl is not similar to anatoxin. If we check the contouring of the difference of electrostatic potential at 30 kcal/mol between the

ferruginine and isoarecolone (figure 29), the ferruginine introduced two extra energy differences at the site of hydrogen bonding which is not found in anatoxin. These extra energy differences may affect the electrostatic potential at the hydrogen bonding site and may be the reason why ferruginine is less potent than anatoxin.

E. Cage Atoms

The program CAGECON (Appendix) first read the coordinates of the molecules along with the dummy atoms. Then it calculated the electrostatic potential of every dummy atom. Different dummy atom types in specified energy ranges were then assigned to dummy atoms according to their electrostatic potential. The newly created file was then read back to CHEM-X and by using command “SET ATOM /COLOR” colors were assigned to each type of dummy atom. Finally, by using the command “DISPLAY” result was displayed. A sample command file is shown after the CAGECON program.

Since both the calculations of electrostatic potentials in ARCHEM and cage atom adopt the same function(II-4), we can predict that the results will be very similar. From figure 7 and 21 we can see that they look similar in all areas except around the nitrogen, where there was no 140–160 kcal(red) energy range in the Cage atom picture but this range was present in the ARCHEM representation. In ARCHEM the dummy atoms on the van der Waals surface did not do well in a very crowded area and may cause some dummy atoms to be overlooked. Yet, the difference could be ignored because that area would not be accessible to the receptor surface where reaction took place. Essentially the speed and convenience obtained from the cage atom method is valuable without losing accuracy and the applications for realtime simulations of the dynamics of molecules may become practical.

Chapter IV

Conclusion

The immediate goal of this research was to study the structural flexibility and electrostatic properties of semirigid nicotinic agonists including the isoquinolone, anatoxin, and ferruginine and to compare these results with those of the potent agonist-isoarecolone. The three series discussed have limited conformational flexibility due to the existence of a second ring which nearly 'fixes' the geometry.

The approach of ring searching can give us some clues about the flexibility. For example isoquinolone has 517 conformations generated from RCG5 but only four conformations remained after optimization with molecular mechanics.

From the structural superposition of isoquinolone to isoarecolone we obtained a good fit at NCO but isoquinolone was found to be a weak agonist, which suggests that the vicinity of the acetyl group of isoquinolone somehow 'blocks' the activity of the agonist. The fitting of the enantiomer of isoquinolone showed that only one enantiomer fit well, therefore a complete survey of the structures is important for an accurate result.

Anatoxin did not fit well on isoarecolone at the NCO, but a better fit was observed if the fitting is at the hydrogen bonding site. Here, however, the nitrogen did not fit well. A similar electrostatic potential pattern between the two atoms attached to the nitrogen was found both in anatoxin and in isoarecolone which implied that besides the structural superposition we should also consider the electrostatic potential distribution of the two proposed binding sites. It might be true that the similarity of electrostatic potentials at the binding site is more important than the structural similarity.

We may assume that ferruginine is an active agonist according to the structural

similarity with anatoxin. But the electrostatic potential showed an extra difference in the area of hydrogen bonding site which might be the reason why ferruginine is much less potent than anatoxin.

In summary, the structural similarity is not sufficient to decide the potency of an agonist. A complete structural survey and electrostatic potential pattern must be considered carefully. By probing the conformational energy surface and molecular properties, we can uncover structural and electrostatic features that could account for the potency of an agonist.

Table 2. Coordinate of FERC

		1.000			1.000			1.000						
		90.000	90.000	90.000										
28	1													
	1 FERC													
1	C1	0.63159	0.63331	3.12131	2	5	6	0	0	0	0	0	0.040	1
2	C2	0.63630	-0.87050	3.01856	1	3	7	8	0	0	0	0	-0.019	1
3	C3	0.46852	-1.32743	1.56068	2	4	9	10	0	0	0	0	0.011	1
4	C4	1.72009	-1.00448	0.71607	3	13	14	15	0	0	0	0	-0.045	1
5	C5	0.37902	1.43539	2.06820	1	11	12	0	0	0	0	0	-0.221	1
6	H6	0.84448	1.03736	4.12609	1	0	0	0	0	0	0	0	0.127	1
7	H7	-0.19014	-1.27327	3.64966	2	0	0	0	0	0	0	0	0.056	1
8	H8	1.58730	-1.27340	3.43847	2	0	0	0	0	0	0	0	0.082	1
9	H9	0.21665	-2.41453	1.51566	3	0	0	0	0	0	0	0	0.090	1
10	N10	-0.56653	-0.51990	0.86394	3	11	24	28	0	0	0	0	-0.041	1
11	C11	0.10055	0.80110	0.72481	5	10	15	16	0	0	0	0	0.082	1
12	C12	0.40830	2.78728	2.23216	5	17	18	0	0	0	0	0	0.243	1
13	H13	1.85881	-1.77148	-0.08330	4	0	0	0	0	0	0	0	0.054	1
14	H14	2.64925	-0.99077	1.33252	4	0	0	0	0	0	0	0	0.073	1
15	C15	1.43072	0.37232	0.08269	4	11	19	20	0	0	0	0	-0.045	1
16	H16	-0.52298	1.43571	0.05389	11	0	0	0	0	0	0	0	0.089	1
17	O17	0.65445	3.29346	3.30106	12	0	0	0	0	0	0	0	-0.246	1
18	C18	0.17074	3.71102	1.04673	12	21	22	23	0	0	0	0	-0.024	1
19	H19	2.24853	1.11198	0.25309	15	0	0	0	0	0	0	0	0.081	1
20	H20	1.29403	0.26105	-1.02002	15	0	0	0	0	0	0	0	0.046	1
21	H21	0.41371	4.76559	1.31183	18	0	0	0	0	0	0	0	0.053	1
22	H22	0.82001	3.43953	0.18331	18	0	0	0	0	0	0	0	0.009	1
23	H23	-0.90001	3.68467	0.74076	18	0	0	0	0	0	0	0	0.017	1
24	C24	-1.90437	-0.48344	1.50489	10	25	26	27	0	0	0	0	0.083	1
25	H25	-2.60145	0.09329	0.85614	24	0	0	0	0	0	0	0	0.062	1
26	H26	-1.89186	-0.00787	2.51039	24	0	0	0	0	0	0	0	0.071	1
27	H27	-2.29784	-1.52086	1.59649	24	0	0	0	0	0	0	0	0.062	1
28	H28	-0.68364	-0.91728	-0.08125	10	0	0	0	0	0	0	0	0.211	1

Table 3. Coordinate of FERF

				1.000	1.000	1.000								
				90.000	90.000	90.000								
28	1													
	1	FERF												
1	C1	0.47140	-1.91365	2.07128	2	5	6	0	0	0	0	0	0.037	1
2	C2	0.51978	-3.41807	2.16711	1	3	7	8	0	0	0	0	-0.032	1
3	C3	0.29049	-4.08254	0.79793	2	4	9	10	0	0	0	0	0.009	1
4	C4	1.46788	-3.84381	-0.16919	3	13	14	15	0	0	0	0	-0.034	1
5	C5	0.12918	-1.26839	0.93904	1	11	12	0	0	0	0	0	-0.229	1
6	H6	0.73888	-1.37183	2.99500	1	0	0	0	0	0	0	0	0.128	1
7	H7	-0.27894	-3.73759	2.87745	2	0	0	0	0	0	0	0	0.054	1
8	H8	1.49823	-3.74157	2.59304	2	0	0	0	0	0	0	0	0.084	1
9	H9	0.07821	-5.16931	0.94621	3	0	0	0	0	0	0	0	0.092	1
10	N10	-0.85794	-3.37182	0.17362	3	11	24	28	0	0	0	0	-0.041	1
11	C11	-0.21143	-2.10571	-0.27066	5	10	15	16	0	0	0	0	0.079	1
12	C12	0.14056	0.09324	0.90729	5	17	18	0	0	0	0	0	0.244	1
13	H13	1.57974	-4.70285	-0.87295	4	0	0	0	0	0	0	0	0.054	1
14	H14	2.43388	-3.73344	0.37681	4	0	0	0	0	0	0	0	0.072	1
15	C15	1.09543	-2.56292	-0.94088	4	11	19	20	0	0	0	0	-0.034	1
16	H16	-0.90664	-1.56915	-0.95637	11	0	0	0	0	0	0	0	0.088	1
17	O17	0.45036	0.74769	1.87421	12	0	0	0	0	0	0	0	-0.245	1
18	C18	-0.19712	0.83541	-0.37734	12	21	22	23	0	0	0	0	-0.024	1
19	H19	1.89339	-1.78453	-0.89345	15	0	0	0	0	0	0	0	0.078	1
20	H20	0.92078	-2.79030	-2.01936	15	0	0	0	0	0	0	0	0.048	1
21	H21	0.04584	1.91876	-0.28379	18	0	0	0	0	0	0	0	0.053	1
22	H22	0.39308	0.44737	-1.23863	18	0	0	0	0	0	0	0	0.009	1
23	H23	-1.28625	0.75755	-0.59756	18	0	0	0	0	0	0	0	0.018	1
24	C24	-1.47916	-4.14025	-0.93725	10	25	26	27	0	0	0	0	0.085	1
25	H25	-2.29918	-3.54018	-1.39235	24	0	0	0	0	0	0	0	0.063	1
26	H26	-1.93218	-5.07217	-0.52991	24	0	0	0	0	0	0	0	0.061	1
27	H27	-0.74989	-4.41772	-1.73052	24	0	0	0	0	0	0	0	0.071	1
28	H28	-1.57212	-3.17046	0.88831	10	0	0	0	0	0	0	0	0.214	1

Table 4. Coordinate of FERH

		90.000			1.000			1.000			1.000		
25 1 FERH		90.000	90.000	90.000	90.000	90.000	90.000	90.000	90.000	90.000	90.000	90.000	
1	C1	0.15357	-1.58056	1.90294	2	5	6	0	0	0	0	0.038	1
2	C2	0.21686	-3.06671	2.15591	1	3	7	8	0	0	0	-0.028	1
3	C3	0.27709	-3.84945	0.83519	2	4	9	10	0	0	0	0.006	1
4	C4	1.58579	-3.61074	0.05732	3	13	14	15	0	0	0	-0.039	1
5	C5	-0.00811	-1.05570	0.67210	1	11	12	0	0	0	0	-0.225	1
6	H6	0.25247	-0.94504	2.79998	1	0	0	0	0	0	0	0.130	1
7	H7	-0.69395	-3.35805	2.73030	2	0	0	0	0	0	0	0.057	1
8	H8	1.10615	-3.30977	2.78324	2	0	0	0	0	0	0	0.087	1
9	H9	0.07786	-4.93411	1.00806	3	0	0	0	0	0	0	0.094	1
10	N10	-0.75732	-3.27086	-0.05052	3	11	24	25	0	0	0	-0.005	1
11	C11	-0.13403	-2.00393	-0.49422	5	10	15	16	0	0	0	0.079	1
12	C12	-0.02088	0.29666	0.51022	5	17	18	0	0	0	0	0.243	1
13	H13	1.89832	-4.53355	-0.48747	4	0	0	0	0	0	0	0.060	1
14	H14	2.41895	-3.32163	0.73995	4	0	0	0	0	0	0	0.072	1
15	C15	1.25261	-2.48654	-0.94271	4	11	19	20	0	0	0	-0.040	1
16	H16	-0.75959	-1.59602	-1.32084	11	0	0	0	0	0	0	0.091	1
17	O17	0.10860	1.04931	1.44600	12	0	0	0	0	0	0	-0.243	1
18	C18	-0.15965	0.90081	-0.87929	12	21	22	23	0	0	0	-0.024	1
19	H19	2.01288	-1.67005	-0.95261	15	0	0	0	0	0	0	0.085	1
20	H20	1.18185	-2.90571	-1.97528	15	0	0	0	0	0	0	0.047	1
21	H21	0.04998	1.99489	-0.85762	18	0	0	0	0	0	0	0.054	1
22	H22	0.56444	0.44882	-1.59476	18	0	0	0	0	0	0	0.008	1
23	H23	-1.19858	0.76875	-1.25862	18	0	0	0	0	0	0	0.019	1
24	H24	-1.64420	-3.11658	0.44536	10	0	0	0	0	0	0	0.216	1
25	H25	-0.94792	-3.89087	-0.84823	10	0	0	0	0	0	0	0.217	1

Table 5. Coordinate of FERN

		1.000			1.000			1.000						
		90.000	90.000	90.000										
31	1 FERN													
	1													
1	C1	0.68110	-2.05662	1.51097	2	5	6	0	0	0	0	0	0.039	1
2	C2	0.61088	-3.56035	1.59640	1	3	7	8	0	0	0	0	-0.022	1
3	C3	0.55968	-4.19857	0.19394	2	4	9	10	0	0	0	0	0.017	1
4	C4	1.94037	-4.04742	-0.49136	3	13	14	15	0	0	0	0	-0.040	1
5	C5	0.58663	-1.39340	0.34124	1	11	12	0	0	0	0	0	-0.226	1
6	H6	0.80254	-1.53259	2.47468	1	0	0	0	0	0	0	0	0.125	1
7	H7	-0.29186	-3.84425	2.18634	2	0	0	0	0	0	0	0	0.053	1
8	H8	1.48814	-3.94456	2.16728	2	0	0	0	0	0	0	0	0.080	1
9	H9	0.26226	-5.27148	0.28990	3	0	0	0	0	0	0	0	0.087	1
10	N10	-0.36869	-3.44391	-0.70930	3	11	24	25	0	0	0	0	-0.077	1
11	C11	0.43708	-2.20015	-0.93365	5	10	15	16	0	0	0	0	0.085	1
12	C12	0.67377	-0.03409	0.33329	5	17	18	0	0	0	0	0	0.243	1
13	H13	2.14607	-4.90637	-1.17328	4	0	0	0	0	0	0	0	0.050	1
14	H14	2.77819	-4.02318	0.24401	4	0	0	0	0	0	0	0	0.069	1
15	C15	1.84420	-2.72688	-1.28429	4	11	19	20	0	0	0	0	-0.037	1
16	H16	-0.02974	-1.60795	-1.75415	11	0	0	0	0	0	0	0	0.085	1
17	O17	0.83296	0.59877	1.35006	12	0	0	0	0	0	0	0	-0.249	1
18	C18	0.61525	0.73560	-0.97787	12	21	22	23	0	0	0	0	-0.024	1
19	H19	2.65004	-2.00540	-1.00973	15	0	0	0	0	0	0	0	0.075	1
20	H20	1.94259	-2.90785	-2.38076	15	0	0	0	0	0	0	0	0.047	1
21	H21	0.87065	1.80841	-0.81885	18	0	0	0	0	0	0	0	0.052	1
22	H22	1.34928	0.33780	-1.71529	18	0	0	0	0	0	0	0	0.010	1
23	H23	-0.41272	0.70035	-1.40555	18	0	0	0	0	0	0	0	0.016	1
24	C24	-1.72202	-3.17337	-0.12587	10	26	27	28	0	0	0	0	0.089	1
25	C25	-0.59395	-4.19709	-1.99120	10	29	30	31	0	0	0	0	0.088	1
26	H26	-2.35033	-2.60350	-0.84841	24	0	0	0	0	0	0	0	0.061	1
27	H27	-1.69422	-2.56529	0.80354	24	0	0	0	0	0	0	0	0.062	1
28	H28	-2.24067	-4.12938	0.11631	24	0	0	0	0	0	0	0	0.060	1
29	H29	-1.19747	-3.59016	-2.70478	25	0	0	0	0	0	0	0	0.060	1
30	H30	-1.14551	-5.14538	-1.79531	25	0	0	0	0	0	0	0	0.060	1
31	H31	0.34287	-4.47804	-2.51784	25	0	0	0	0	0	0	0	0.063	1

Table 7. Coordinate of ANAN

				1.000	1.000	1.000								
				90.000	90.000	90.000								
34	1	ANAN												
1														
1	C1	0.00000	0.00000	0.00000	2	5	6	0	0	0	0	0.054		
2	C2	0.56370	-1.34543	-0.37888	1	7	8	26	0	0	0	-0.022		
3	C3	-1.18865	-1.89528	-2.34526	4	9	10	26	0	0	0	0.030		
4	C4	-1.18115	-0.97646	-3.59197	3	13	14	15	0	0	0	-0.044		
5	C5	-1.08570	0.64392	-0.47460	1	11	12	0	0	0	0	-0.239		
6	H6	0.57672	0.47849	0.81188	1	0	0	0	0	0	0	0.105		
7	H7	0.33143	-2.09760	0.40932	2	0	0	0	0	0	0	0.045		
8	H8	1.67510	-1.24755	-0.31432	2	0	0	0	0	0	0	0.057		
9	H9	-1.44148	-2.94315	-2.64021	3	0	0	0	0	0	0	0.077		
10	N10	-2.30776	-1.31838	-1.52457	3	11	24	25	0	0	0	-0.070		
11	C11	-2.01352	0.14855	-1.56482	5	10	15	16	0	0	0	0.097		
12	C12	-1.39089	1.84683	0.09015	5	17	18	0	0	0	0	0.240		
13	H13	-1.97329	-1.26738	-4.31984	4	0	0	0	0	0	0	0.040		
14	H14	-0.24536	-1.00818	-4.19795	4	0	0	0	0	0	0	0.075		
15	C15	-1.44868	0.41118	-2.98020	4	11	19	20	0	0	0	-0.036		
16	H16	-2.98627	0.67626	-1.42268	11	0	0	0	0	0	0	0.066		
17	O17	-1.24761	2.02567	1.27678	12	0	0	0	0	0	0	-0.252		
18	C18	-1.99071	2.97170	-0.74043	12	21	22	23	0	0	0	-0.022		
19	H19	-0.49745	0.99112	-2.92238	15	0	0	0	0	0	0	0.061		
20	H20	-2.16030	0.99213	-3.61412	15	0	0	0	0	0	0	0.059		
21	H21	-1.59451	3.95302	-0.39261	18	0	0	0	0	0	0	0.049		
22	H22	-1.73490	2.88952	-1.82024	18	0	0	0	0	0	0	0.002		
23	H23	-3.09857	2.98918	-0.62572	18	0	0	0	0	0	0	0.028		
24	C24	-2.50212	-1.90058	-0.15810	10	32	33	34	0	0	0	0.089		
25	C25	-3.63084	-1.56724	-2.21918	10	29	30	31	0	0	0	0.082		
26	C26	0.24974	-1.89065	-1.77119	2	3	27	28	0	0	0	-0.027		
27	H27	0.64075	-2.93627	-1.81359	26	0	0	0	0	0	0	0.050		
28	H28	0.92691	-1.33330	-2.45893	26	0	0	0	0	0	0	0.043		
29	H29	-4.48352	-1.16419	-1.62495	25	0	0	0	0	0	0	0.059		
30	H30	-3.81011	-2.65833	-2.35977	25	0	0	0	0	0	0	0.062		
31	H31	-3.72238	-1.07474	-3.21085	25	0	0	0	0	0	0	0.062		
32	H32	-3.38767	-1.44742	0.34399	24	0	0	0	0	0	0	0.061		
33	H33	-1.66957	-1.72719	0.54495	24	0	0	0	0	0	0	0.062		
34	H34	-2.65486	-3.00246	-0.22230	24	0	0	0	0	0	0	0.059		

Table 8. Coordinate of ANAC

				1.000	1.000	1.000								
				90.000	90.000	90.000								
31	1	ANAC												
1														
1	C1	0.00000	0.00000	0.00000	2	5	6	0	0	0	0	0.055		
2	C2	0.20769	-1.45366	-0.35418	1	7	8	26	0	0	0	-0.025		
3	C3	-1.51353	-1.63262	-2.34254	4	9	10	26	0	0	0	0.019		
4	C4	-1.43828	-0.77157	-3.62134	3	13	14	15	0	0	0	-0.052		
5	C5	-0.85950	0.89428	-0.53201	1	11	12	0	0	0	0	-0.235		
6	H6	0.65215	0.32672	0.82947	1	0	0	0	0	0	0	0.109		
7	H7	-0.32370	-2.11647	0.36557	2	0	0	0	0	0	0	0.044		
8	H8	1.29005	-1.67032	-0.18166	2	0	0	0	0	0	0	0.061		
9	H9	-2.02094	-2.60654	-2.54543	3	0	0	0	0	0	0	0.085		
10	N10	-2.43477	-0.75495	-1.57895	3	11	24	25	0	0	0	-0.034		
11	C11	-1.83809	0.60099	-1.64541	5	10	15	16	0	0	0	0.094		
12	C12	-0.86712	2.15488	-0.01326	5	17	18	0	0	0	0	0.239		
13	H13	-2.41615	-0.81603	-4.15989	4	0	0	0	0	0	0	0.036		
14	H14	-0.64753	-1.09097	-4.34080	4	0	0	0	0	0	0	0.084		
15	C15	-1.21929	0.64698	-3.05767	4	11	19	20	0	0	0	-0.041		
16	H16	-2.71179	1.29063	-1.57361	11	0	0	0	0	0	0	0.068		
17	O17	-0.63862	2.34944	1.15719	12	0	0	0	0	0	0	-0.250		
18	C18	-1.23165	3.34963	-0.88199	12	21	22	23	0	0	0	-0.022		
19	H19	-0.13054	0.88290	-3.00241	15	0	0	0	0	0	0	0.062		
20	H20	-1.69926	1.41587	-3.70891	15	0	0	0	0	0	0	0.067		
21	H21	-0.66090	4.24864	-0.55476	18	0	0	0	0	0	0	0.051		
22	H22	-0.98062	3.18579	-1.95386	18	0	0	0	0	0	0	0.002		
23	H23	-2.31723	3.58056	-0.78747	18	0	0	0	0	0	0	0.027		
24	C24	-2.94812	-1.20279	-0.26144	10	29	30	31	0	0	0	0.084		
25	H25	-3.28269	-0.70626	-2.17122	10	0	0	0	0	0	0	0.200		
26	C26	-0.09044	-1.85217	-1.79797	2	3	27	28	0	0	0	-0.022		
27	H27	0.15996	-2.93339	-1.92275	26	0	0	0	0	0	0	0.058		
28	H28	0.65508	-1.32200	-2.43539	26	0	0	0	0	0	0	0.045		
29	H29	-3.78782	-0.53475	0.03507	24	0	0	0	0	0	0	0.060		
30	H30	-2.20298	-1.17427	0.55769	24	0	0	0	0	0	0	0.073		
31	H31	-3.35173	-2.23609	-0.35307	24	0	0	0	0	0	0	0.061		

Table 10. Coordinate of ME1Z

		1.000			1.000			1.000						
		90.000	90.000	90.000										
33	1 MET1Z													
	1													
1	C1	-0.15780	0.89160	-0.76400	2	3	4	14	0	0	0	0	0.000	1
2	C2	0.43280	0.66060	0.63080	1	5	13	33	0	0	0	0	0.000	1
3	C3	0.05700	-0.36140	-1.63750	1	6	15	16	0	0	0	0	0.000	1
4	C4	0.37710	2.17590	-1.39070	1	7	8	0	0	0	0	0	0.000	1
5	C5	-0.16940	-0.57880	1.33250	2	9	17	18	0	0	0	0	0.000	1
6	C6	0.28650	-1.65110	-0.82630	3	9	19	20	0	0	0	0	0.000	1
7	C7	0.31270	3.42000	-0.52470	4	12	21	22	0	0	0	0	0.000	1
8	O8	0.79180	2.19390	-2.52500	4	0	0	0	0	0	0	0	0.000	1
9	N9	-0.53900	-1.71660	0.41990	5	6	10	11	0	0	0	0	0.000	1
10	C10	-2.00080	-1.69100	0.07650	9	23	24	25	0	0	0	0	0.000	1
11	C11	-0.27760	-3.01920	1.12190	9	26	27	28	0	0	0	0	0.000	1
12	C12	0.94640	3.14490	0.84490	7	13	29	30	0	0	0	0	0.000	1
13	C13	0.30700	1.91740	1.51200	2	12	31	32	0	0	0	0	0.000	1
14	H14	-1.24790	1.08770	-0.64040	1	0	0	0	0	0	0	0	0.000	1
15	H15	-0.80990	-0.48190	-2.33040	3	0	0	0	0	0	0	0	0.000	1
16	H16	0.95230	-0.23620	-2.29090	3	0	0	0	0	0	0	0	0.000	1
17	H17	-1.05390	-0.29820	1.94990	5	0	0	0	0	0	0	0	0.000	1
18	H18	0.60260	-0.91200	2.06600	5	0	0	0	0	0	0	0	0.000	1
19	H19	1.36430	-1.72140	-0.54370	6	0	0	0	0	0	0	0	0.000	1
20	H20	0.08010	-2.53440	-1.47710	6	0	0	0	0	0	0	0	0.000	1
21	H21	0.83400	4.26590	-1.03210	7	0	0	0	0	0	0	0	0.000	1
22	H22	-0.75910	3.70370	-0.40620	7	0	0	0	0	0	0	0	0.000	1
23	H23	-2.31280	-0.74080	-0.40540	10	0	0	0	0	0	0	0	0.000	1
24	H24	-2.62820	-1.81150	0.98960	10	0	0	0	0	0	0	0	0.000	1
25	H25	-2.26000	-2.51960	-0.62220	10	0	0	0	0	0	0	0	0.000	1
26	H26	0.80270	-3.13490	1.37110	11	0	0	0	0	0	0	0	0.000	1
27	H27	-0.56470	-3.88610	0.48290	11	0	0	0	0	0	0	0	0.000	1
28	H28	-0.85780	-3.08380	2.07170	11	0	0	0	0	0	0	0	0.000	1
29	H29	0.82960	4.04030	1.50180	12	0	0	0	0	0	0	0	0.000	1
30	H30	2.04190	2.97110	0.71940	12	0	0	0	0	0	0	0	0.000	1
31	H31	0.79170	1.73510	2.50100	13	0	0	0	0	0	0	0	0.000	1
32	H32	-0.77080	2.12910	1.70760	13	0	0	0	0	0	0	0	0.000	1
33	H33	1.52570	0.47950	0.47910	2	0	0	0	0	0	0	0	0.000	1

Table 11. Coordinate of MET4Z

				1.000	1.000	1.000								
				90.000	90.000	90.000								
33	1	MET4Z												
1														
1	C1	-0.55820	1.27550	-0.62070	2	3	4	14	0	0	0	0	0.000	1
2	C2	0.22740	0.78760	0.61380	1	5	13	33	0	0	0	0	0.000	1
3	C3	-1.12780	0.10180	-1.44320	1	6	15	16	0	0	0	0	0.000	1
4	C4	0.36500	2.24230	-1.34570	1	7	8	0	0	0	0	0	0.000	1
5	C5	-0.53470	-0.39820	1.21840	2	9	17	18	0	0	0	0	0.000	1
6	C6	-0.37090	-1.19450	-1.13130	3	9	19	20	0	0	0	0	0.000	1
7	C7	0.74990	3.46300	-0.52590	4	12	21	22	0	0	0	0	0.000	1
8	O8	0.75780	2.01310	-2.46430	4	0	0	0	0	0	0	0	0.000	1
9	N9	-0.49290	-1.60210	0.31410	5	6	10	11	0	0	0	0	0.000	1
10	C10	-1.73800	-2.41170	0.52830	9	23	24	25	0	0	0	0	0.000	1
11	C11	0.68340	-2.47060	0.65590	9	26	27	28	0	0	0	0	0.000	1
12	C12	1.32060	3.04640	0.84140	7	13	29	30	0	0	0	0	0.000	1
13	C13	0.45930	1.98340	1.55240	2	12	31	32	0	0	0	0	0.000	1
14	H14	-1.43140	1.89360	-0.29990	1	0	0	0	0	0	0	0	0.000	1
15	H15	-2.20620	-0.04900	-1.20050	3	0	0	0	0	0	0	0	0.000	1
16	H16	-1.09960	0.32400	-2.53570	3	0	0	0	0	0	0	0	0.000	1
17	H17	-1.58540	-0.05480	1.36600	5	0	0	0	0	0	0	0	0.000	1
18	H18	-0.15530	-0.65670	2.23460	5	0	0	0	0	0	0	0	0.000	1
19	H19	0.69600	-1.01060	-1.40020	6	0	0	0	0	0	0	0	0.000	1
20	H20	-0.70200	-2.02540	-1.79860	6	0	0	0	0	0	0	0	0.000	1
21	H21	1.48790	4.08320	-1.08750	7	0	0	0	0	0	0	0	0.000	1
22	H22	-0.16770	4.08010	-0.38260	7	0	0	0	0	0	0	0	0.000	1
23	H23	-2.64970	-1.83910	0.24280	10	0	0	0	0	0	0	0	0.000	1
24	H24	-1.83990	-2.70690	1.59830	10	0	0	0	0	0	0	0	0.000	1
25	H25	-1.72340	-3.34370	-0.08250	10	0	0	0	0	0	0	0	0.000	1
26	H26	1.64160	-1.90870	0.57020	11	0	0	0	0	0	0	0	0.000	1
27	H27	0.73900	-3.35220	-0.02390	11	0	0	0	0	0	0	0	0.000	1
28	H28	0.61250	-2.85170	1.70080	11	0	0	0	0	0	0	0	0.000	1
29	H29	1.43430	3.94450	1.49500	12	0	0	0	0	0	0	0	0.000	1
30	H30	2.34540	2.63130	0.68650	12	0	0	0	0	0	0	0	0.000	1
31	H31	0.97530	1.64280	2.48180	13	0	0	0	0	0	0	0	0.000	1
32	H32	-0.51710	2.42400	1.86340	13	0	0	0	0	0	0	0	0.000	1
33	H33	1.23930	0.42400	0.31260	2	0	0	0	0	0	0	0	0.000	1

Table 12. Coordinate of MET5Z

		1.000			1.000			1.000						
		90.000	90.000	90.000										
33	1 MET5Z													
	1													
1	C1	-0.62460	-0.28115	-0.01108	4	9	13	14	0	0	0	0	-0.060	1
2	C2	1.00118	-0.85775	1.83128	5	10	13	15	0	0	0	0	-0.024	1
3	C3	0.70852	1.55785	1.03699	6	13	27	0	0	0	0	0	0.227	1
4	C4	-0.63118	-1.76943	-0.41048	1	7	17	18	0	0	0	0	0.066	1
5	C5	0.94750	-2.32651	1.38190	2	7	19	20	0	0	0	0	0.051	1
6	C6	0.40074	2.52551	-0.09049	3	8	22	23	0	0	0	0	-0.047	1
7	N7	-0.34905	-2.70567	0.72845	4	5	25	26	0	0	0	0	-0.079	1
8	C8	-0.90179	2.12010	-0.79487	6	9	21	24	0	0	0	0	-0.014	1
9	C9	-0.87953	0.64162	-1.21844	1	8	11	12	0	0	0	0	-0.007	1
10	H10	0.27773	-0.67507	2.65891	2	0	0	0	0	0	0	0	0.044	1
11	H11	-0.08489	0.48785	-1.98620	9	0	0	0	0	0	0	0	0.023	1
12	H12	-1.85278	0.37785	-1.69733	9	0	0	0	0	0	0	0	0.028	1
13	C13	0.71317	0.08425	0.65195	1	2	3	16	0	0	0	0	-0.098	1
14	H14	-1.44819	-0.09306	0.71758	1	0	0	0	0	0	0	0	0.041	1
15	H15	2.01417	-0.63916	2.24760	2	0	0	0	0	0	0	0	0.075	1
16	H16	1.53468	-0.03441	-0.09468	13	0	0	0	0	0	0	0	0.050	1
17	H17	0.14346	-1.90989	-1.20069	4	0	0	0	0	0	0	0	0.062	1
18	H18	-1.61196	-2.02640	-0.87604	4	0	0	0	0	0	0	0	0.067	1
19	H19	1.14630	-2.99371	2.25438	5	0	0	0	0	0	0	0	0.069	1
20	H20	1.78368	-2.48948	0.66075	5	0	0	0	0	0	0	0	0.062	1
21	H21	-1.76146	2.29137	-0.10358	8	0	0	0	0	0	0	0	0.023	1
22	H22	0.32400	3.56501	0.30725	6	0	0	0	0	0	0	0	0.062	1
23	H23	1.25263	2.49840	-0.80943	6	0	0	0	0	0	0	0	0.040	1
24	H24	-1.06682	2.77049	-1.68740	8	0	0	0	0	0	0	0	0.045	1
25	C25	-1.46925	-2.69301	1.72724	7	28	29	30	0	0	0	0	0.083	1
26	C26	-0.23504	-4.10512	0.19502	7	31	32	33	0	0	0	0	0.084	1
27	O27	0.95029	1.90666	2.16776	3	0	0	0	0	0	0	0	-0.243	1
28	H28	-1.62660	-1.69503	2.18883	25	0	0	0	0	0	0	0	0.065	1
29	H29	-1.26879	-3.40867	2.55751	25	0	0	0	0	0	0	0	0.061	1
30	H30	-2.43061	-2.98887	1.24770	25	0	0	0	0	0	0	0	0.059	1
31	H31	-1.18060	-4.42228	-0.30251	26	0	0	0	0	0	0	0	0.061	1
32	H32	-0.01669	-4.83000	1.01299	26	0	0	0	0	0	0	0	0.062	1
33	H33	0.58472	-4.18660	-0.55557	26	0	0	0	0	0	0	0	0.061	1

Table 13. Coordinate of MET6Z

		1.000			1.000			1.000						
		90.000	90.000	90.000										
33	1 MET6Z													
	1													
1	C1	0.37850	0.49790	-0.93480	2	3	4	14	0	0	0	0	0.000	1
2	C2	1.59280	-0.24620	-0.35270	1	5	13	33	0	0	0	0	0.000	1
3	C3	-0.38800	-0.38900	-1.93750	1	6	15	16	0	0	0	0	0.000	1
4	C4	0.80900	1.86000	-1.47260	1	7	8	0	0	0	0	0	0.000	1
5	C5	1.14150	-1.58700	0.25710	2	9	17	18	0	0	0	0	0.000	1
6	C6	0.17890	-1.81490	-2.02070	3	9	19	20	0	0	0	0	0.000	1
7	C7	1.57950	2.73650	-0.50150	4	12	21	22	0	0	0	0	0.000	1
8	O8	0.53610	2.21440	-2.59440	4	0	0	0	0	0	0	0	0.000	1
9	N9	0.36690	-2.47090	-0.68440	5	6	10	11	0	0	0	0	0.000	1
10	C10	-0.96870	-2.80360	-0.08460	9	23	24	25	0	0	0	0	0.000	1
11	C11	1.10500	-3.76250	-0.89390	9	26	27	28	0	0	0	0	0.000	1
12	C12	2.76850	1.96320	0.08350	7	13	29	30	0	0	0	0	0.000	1
13	C13	2.31460	0.62750	0.69190	2	12	31	32	0	0	0	0	0.000	1
14	H14	-0.31190	0.72960	-0.08830	1	0	0	0	0	0	0	0	0.000	1
15	H15	-1.47120	-0.41910	-1.67190	3	0	0	0	0	0	0	0	0.000	1
16	H16	-0.35750	0.03800	-2.96670	3	0	0	0	0	0	0	0	0.000	1
17	H17	0.52720	-1.35500	1.15780	5	0	0	0	0	0	0	0	0.000	1
18	H18	2.03680	-2.12060	0.65360	5	0	0	0	0	0	0	0	0.000	1
19	H19	1.15690	-1.76960	-2.55570	6	0	0	0	0	0	0	0	0.000	1
20	H20	-0.47940	-2.44280	-2.66790	6	0	0	0	0	0	0	0	0.000	1
21	H21	1.93220	3.66040	-1.01800	7	0	0	0	0	0	0	0	0.000	1
22	H22	0.88230	3.04790	0.31110	7	0	0	0	0	0	0	0	0.000	1
23	H23	-1.56770	-1.88520	0.11040	10	0	0	0	0	0	0	0	0.000	1
24	H24	-0.84840	-3.34060	0.88490	10	0	0	0	0	0	0	0	0.000	1
25	H25	-1.56300	-3.45900	-0.76220	10	0	0	0	0	0	0	0	0.000	1
26	H26	2.11590	-3.57910	-1.32650	11	0	0	0	0	0	0	0	0.000	1
27	H27	0.55210	-4.43300	-1.59180	11	0	0	0	0	0	0	0	0.000	1
28	H28	1.23800	-4.31080	0.06750	11	0	0	0	0	0	0	0	0.000	1
29	H29	3.27800	2.58350	0.85970	12	0	0	0	0	0	0	0	0.000	1
30	H30	3.51600	1.76850	-0.72230	12	0	0	0	0	0	0	0	0.000	1
31	H31	3.20200	0.08270	1.09430	13	0	0	0	0	0	0	0	0.000	1
32	H32	1.63550	0.82810	1.55410	13	0	0	0	0	0	0	0	0.000	1
33	H33	2.32710	-0.44510	-1.17050	2	0	0	0	0	0	0	0	0.000	1

Table 14. Area (Square Angstroms) of Electrostatic Potentials on the van der Waals Surface.

agonist	energy range, kcal/mol						
	0-40	40-60	60-80	80-100	100-120	120-140	140-160
FERC	6.3	15.3	31.3	78.9	65.1	14.0	9.4
FERF	7.1	15.6	32.3	75.7	64.3	17.2	8.5
FERH	5.7	14.9	31.2	66.5	48.8	10.6	14.6
FERN	7.5	16.0	32.9	95.7	72.6	13.2	0.0
ANAH	6.8	14.8	33.1	89.7	42.8	9.6	14.8
ANAN	7.9	16.3	40.8	117.2	62.6	8.8	0.00
ANAC	6.8	15.5	35.8	103.4	53.6	12.3	8.4
ANAF	8.2	16.1	36.1	96.6	58.8	15.4	4.8
NET5Z	7.6	15.6	70.5	68.6	77.3	16.2	0.0

Table 15 Energy vs dihedral angle for Table 16 Energy vs dihedral angle for

FERN

ANAZ16

FERN		
Angle (degree)	Minimized energy (Kcal)	Beer's dis- tance (\AA)
0	17.65	6.25
30	18.58	6.35
60	19.78	6.20
90	19.90	5.87
120	15.96	5.47
150	11.65	5.17
180	10.26	4.98
210	11.60	4.86
240	14.89	4.79
270	18.31	5.03
300	18.62	5.59
330	17.70	6.88
360	17.65	6.25

ANAZ16		
Angle (degree)	Minimized energy (Kcal)	Beer's dis- tance (\AA)
0	46.79	6.17
30	48.45	6.27
60	49.12	6.20
90	49.32	5.98
120	6.66	5.34
150	2.82	4.95
180	1.00	4.53
210	0.51	4.08
240	2.31	3.77
270	5.90	3.91
300	7.88	5.08
330	45.94	5.88
360	46.79	6.17

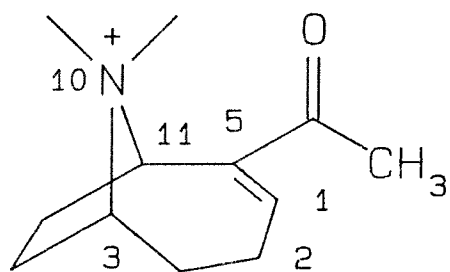
Table 17 Energy vs dihedral angle for Table 18 Energy vs dihedral angle for
 ANAZ84 ANAZ175

ANAZ84		
Angle (degree)	Minimized energy (Kcal)	Beer's dis- tance (\AA)
0	45.27	6.27
30	43.88	6.01
60	44.52	5.67
90	43.65	5.03
120	41.32	5.04
150	38.84	5.13
180	36.04	5.08
210	37.24	5.07
240	41.20	5.08
270	44.84	5.06
300	47.25	5.68
330	46.15	6.13
360	45.27	6.27

ANAZ175		
Angle (degree)	Minimized energy (Kcal)	Beer's dis- tance (\AA)
0	9.40	6.23
30	10.26	6.28
60	11.00	6.13
90	10.61	5.78
120	6.58	5.39
150	2.28	5.09
180	0.95	4.92
210	2.44	4.85
240	5.74	4.85
270	9.11	5.07
300	9.63	5.60
330	9.01	5.99
360	9.40	6.23

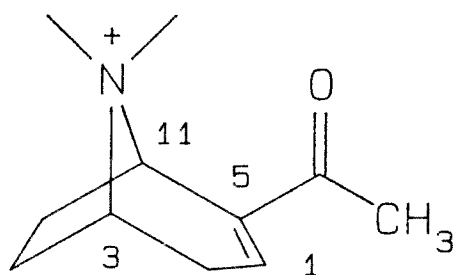
Table 19 Energy vs dihedral angle for ANAZ510

ANAZ510		
Angle (degree)	Minimized energy (Kcal)	Beer's distance (\AA)
0	10.37	6.07
30	10.69	6.26
60	11.33	6.20
90	10.92	5.82
120	6.66	5.34
150	2.82	4.95
180	1.00	4.53
210	0.51	4.08
240	2.31	3.77
270	5.91	3.91
300	7.87	5.07
330	8.75	5.66
360	10.37	6.07



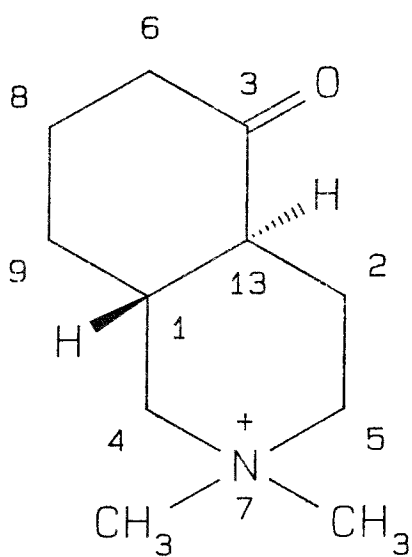
26

I



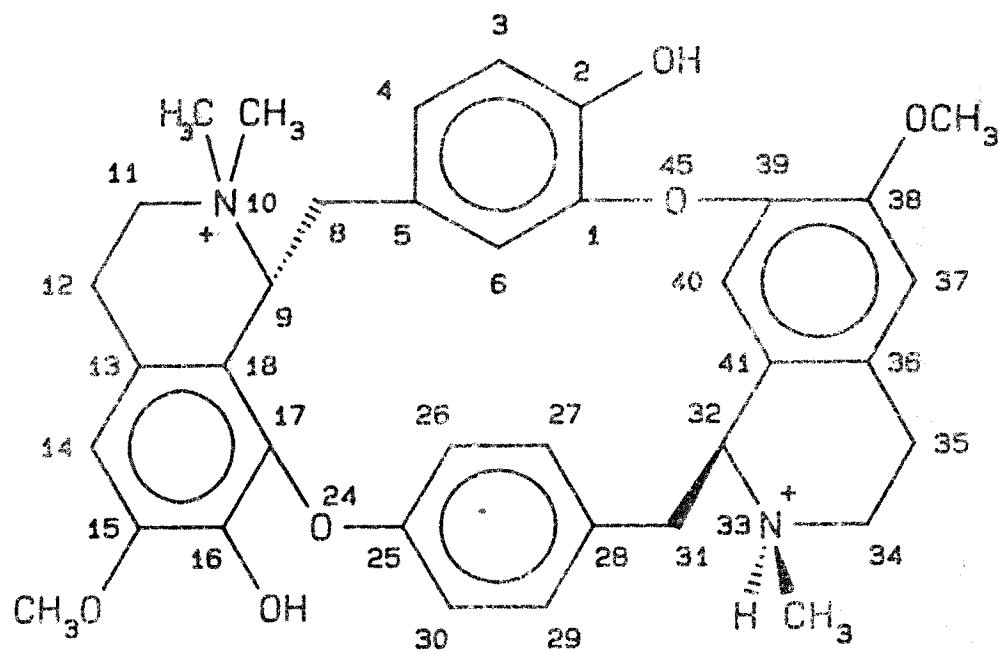
2

II



III

Figure 1. Structure of anatoxin, ferruginine, and isoquinolone.



Tubocurarine

Figure 2

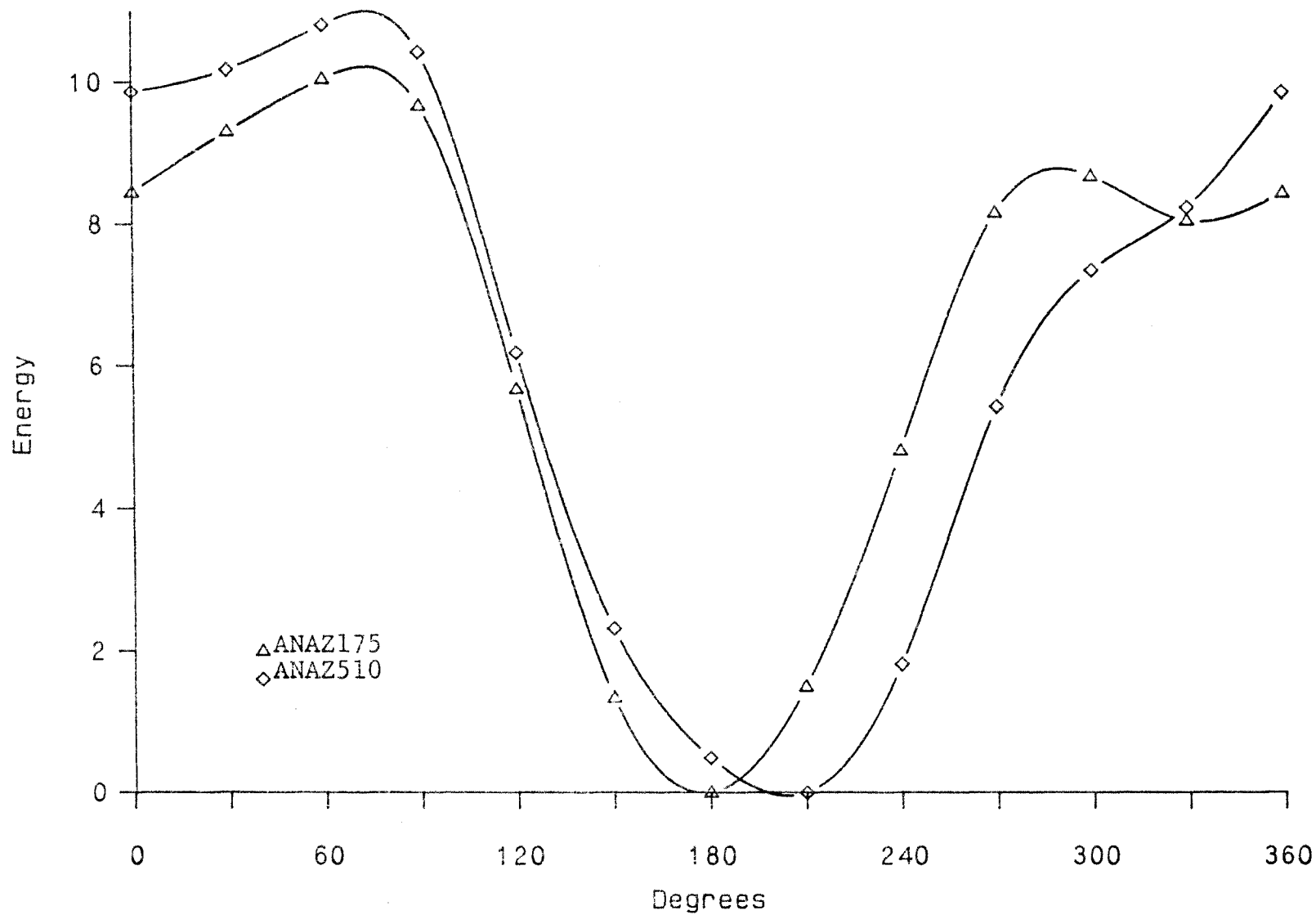


Figure 3. Energy vs dihedral angle for anatoxin series.

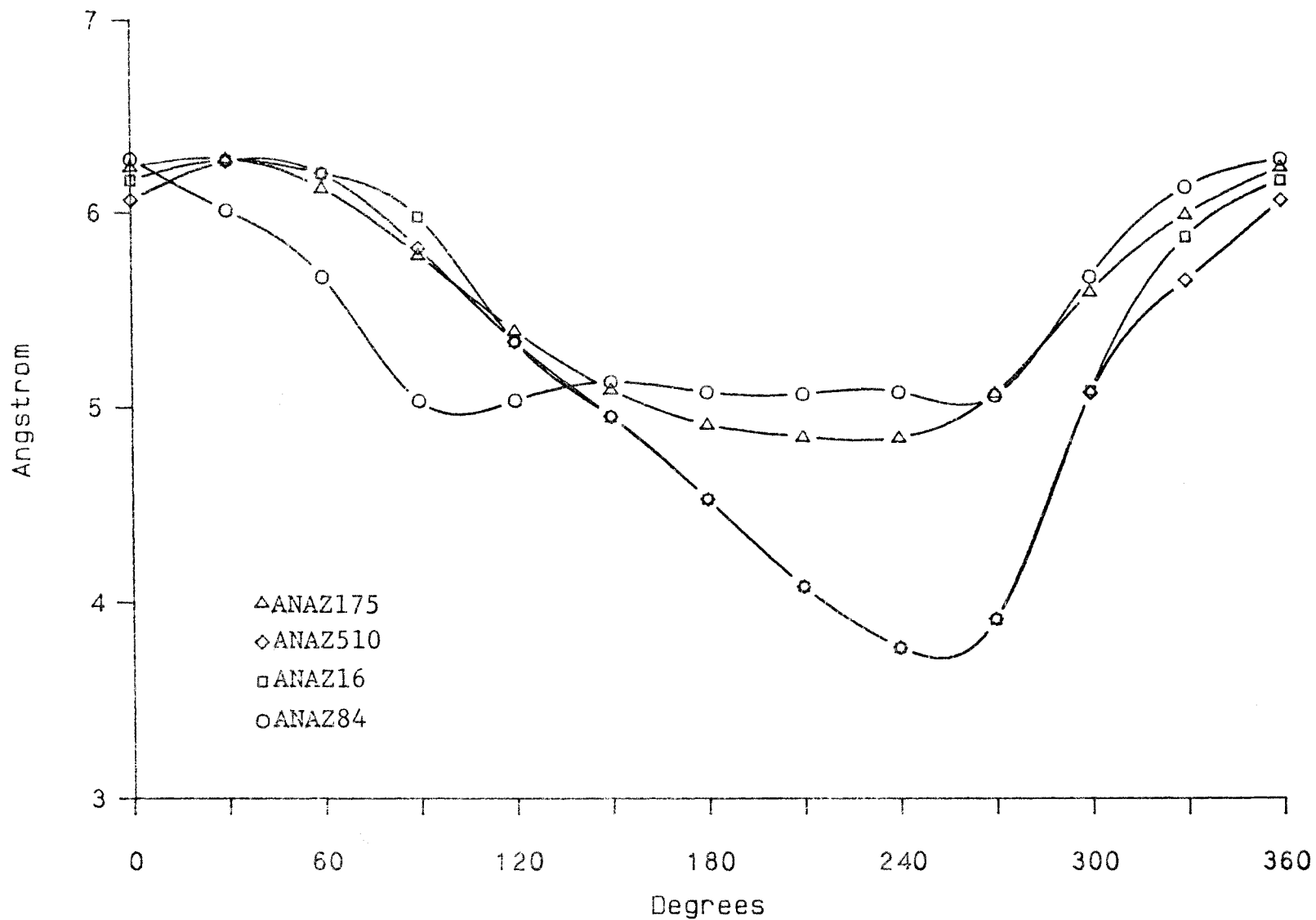


Figure 4. Distance from nitrogen to the van der Waals surface of oxygen vs dihedral angle for anatoxin series.

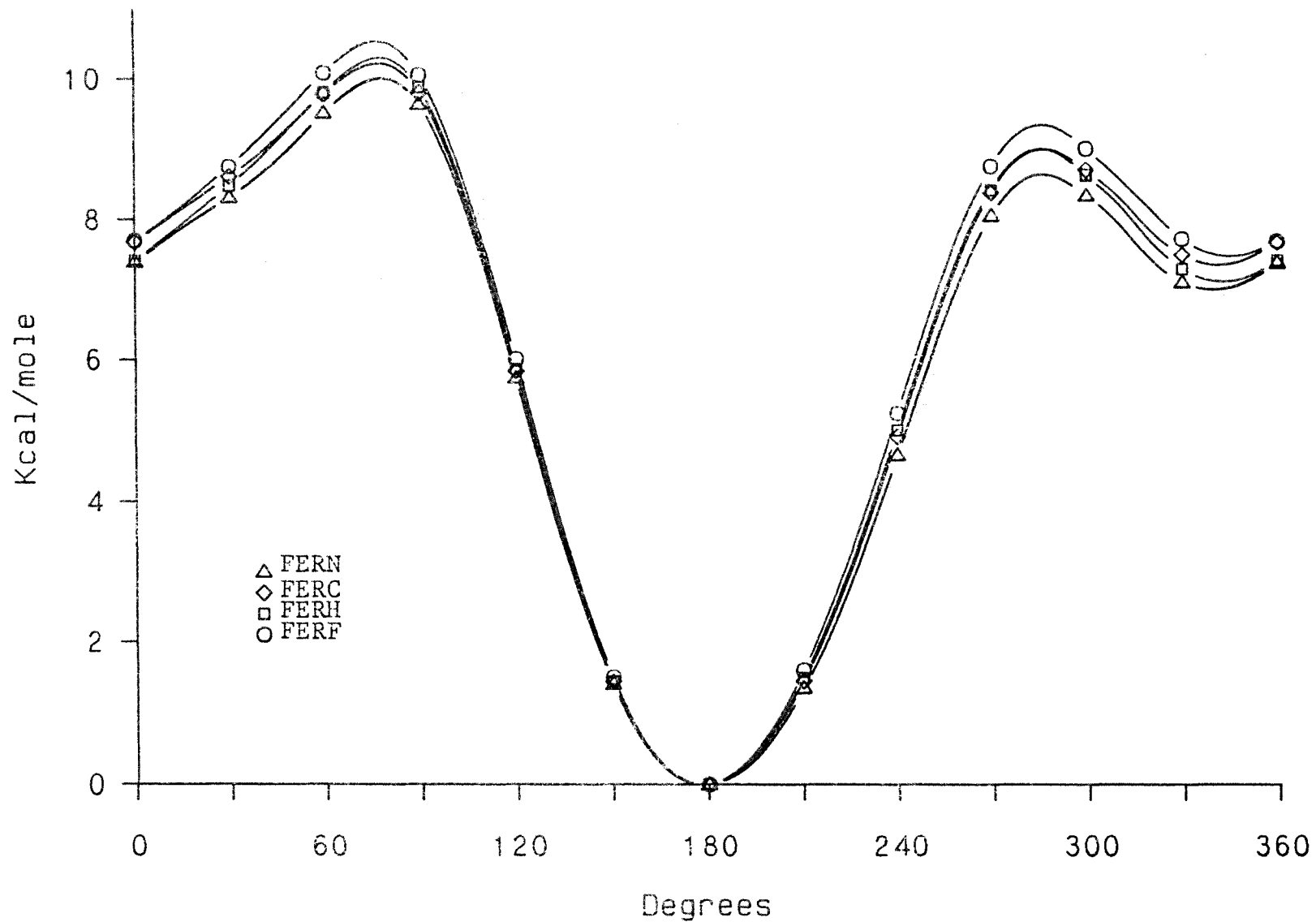


Figure 5. Energy vs dihedral angle for ferruginine series.

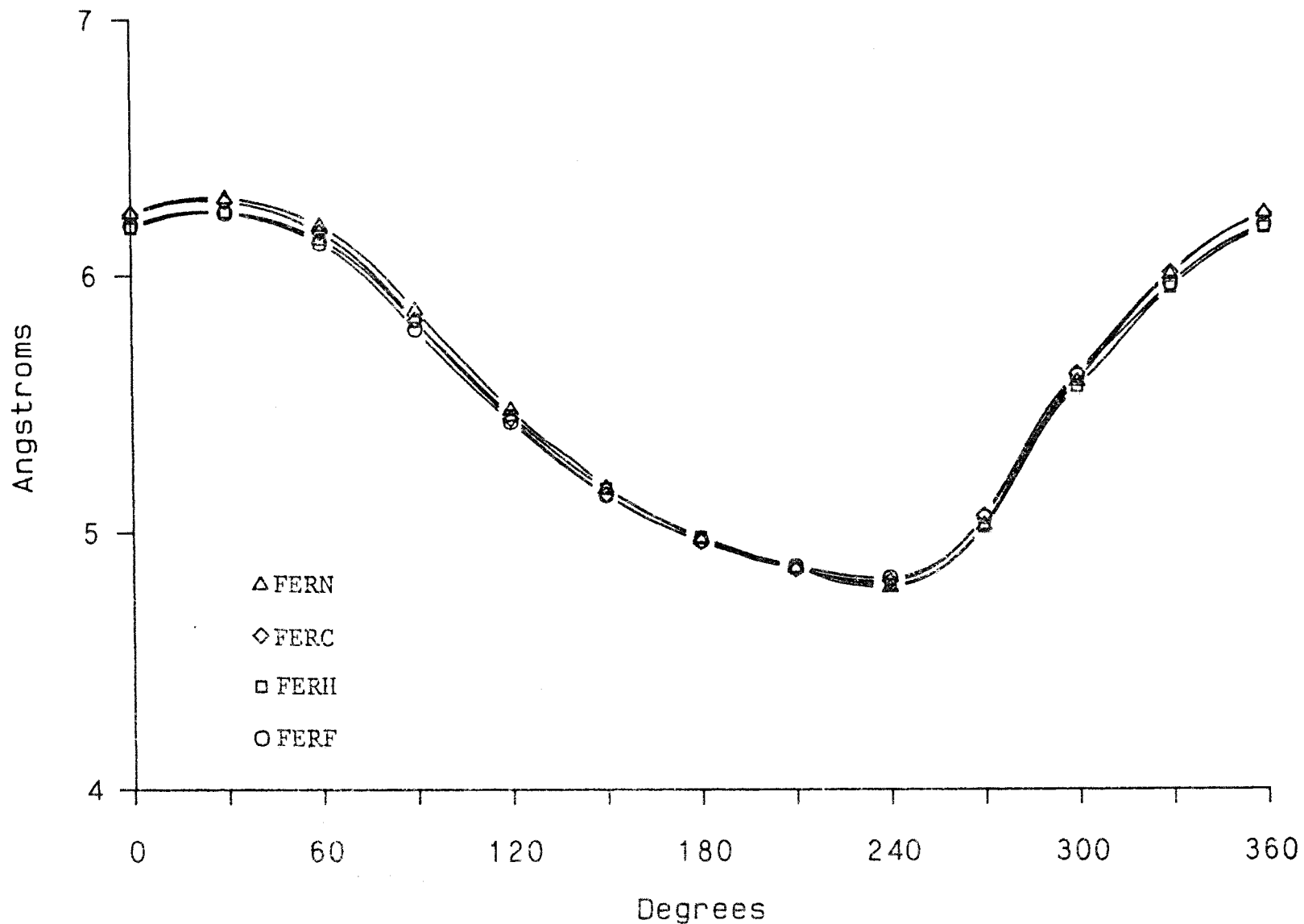


Figure 6. Distance from nitrogen to the van der Waals surface of oxygen vs dihedral angle for ferruginine series.

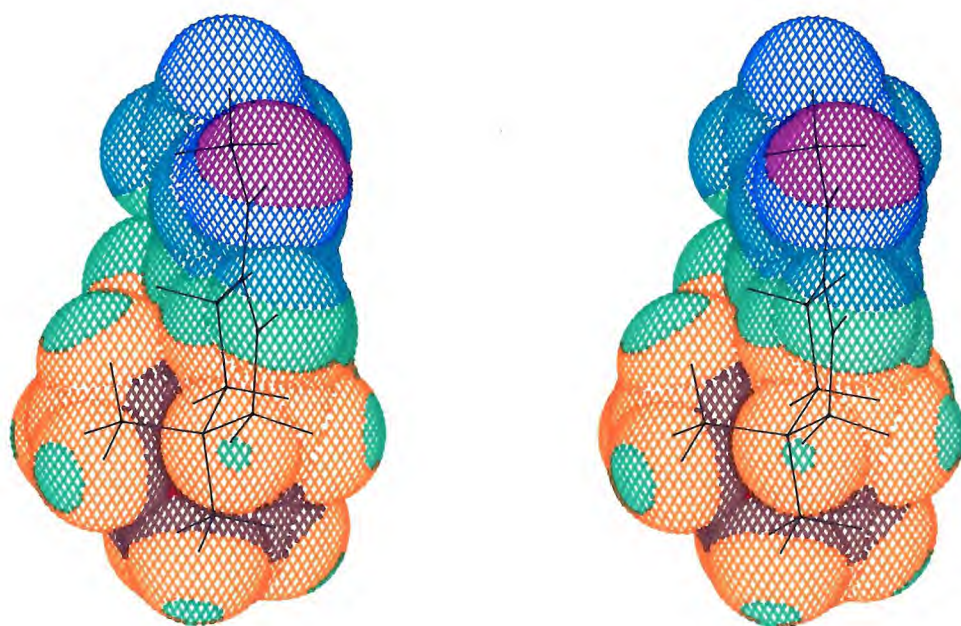


Figure 7. Color coded ESP on van der Waals surface of isoarcalone.

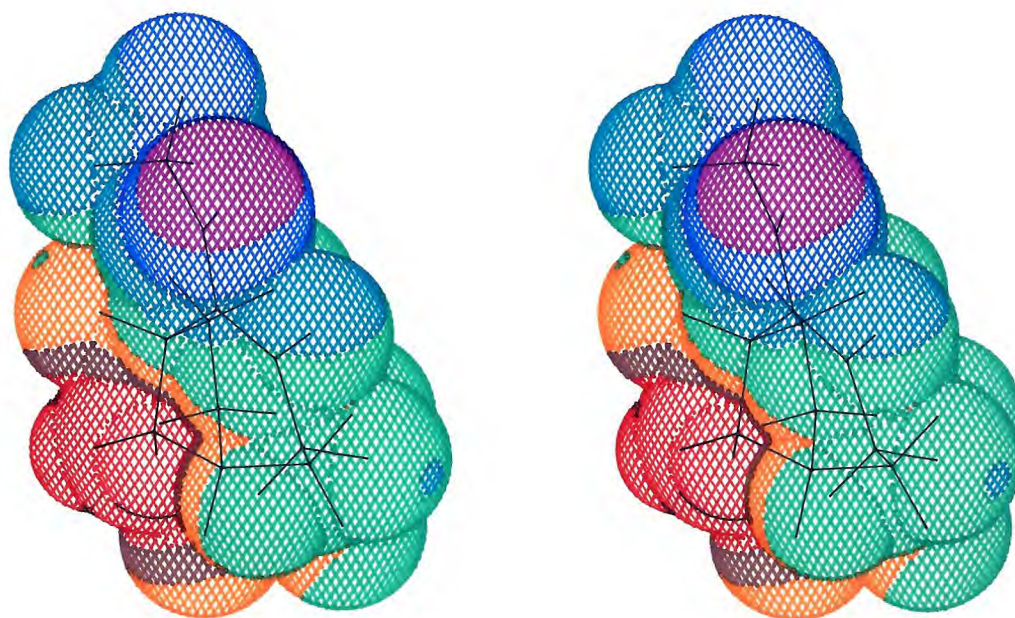


Figure 8. Color coded ESP on van der Waals surface of ANAH.

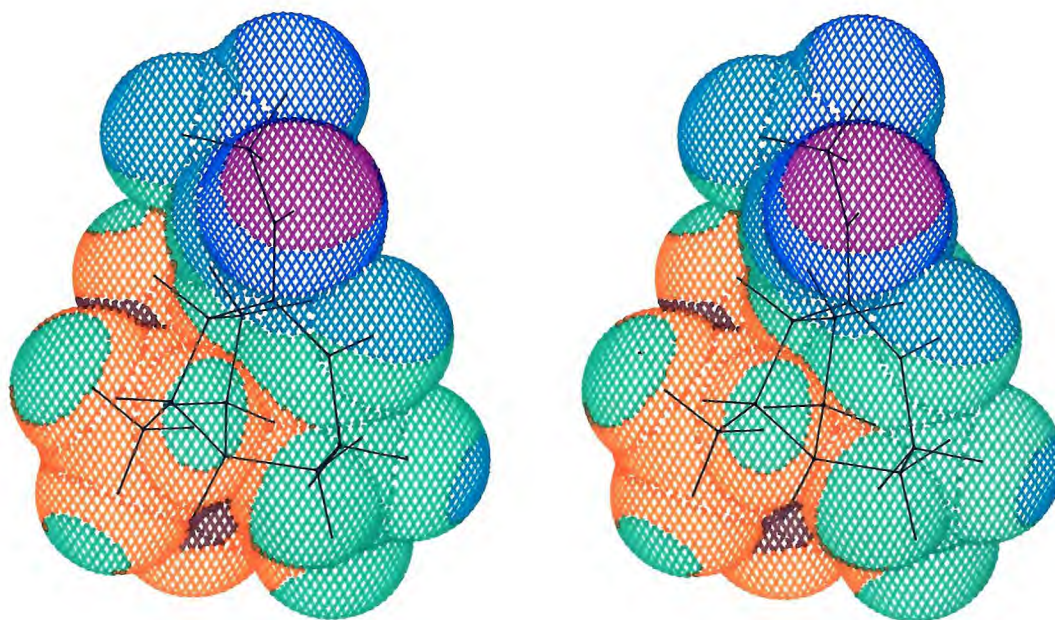


Figure 9. Color coded ESP on van der Waals surface of ANAC.

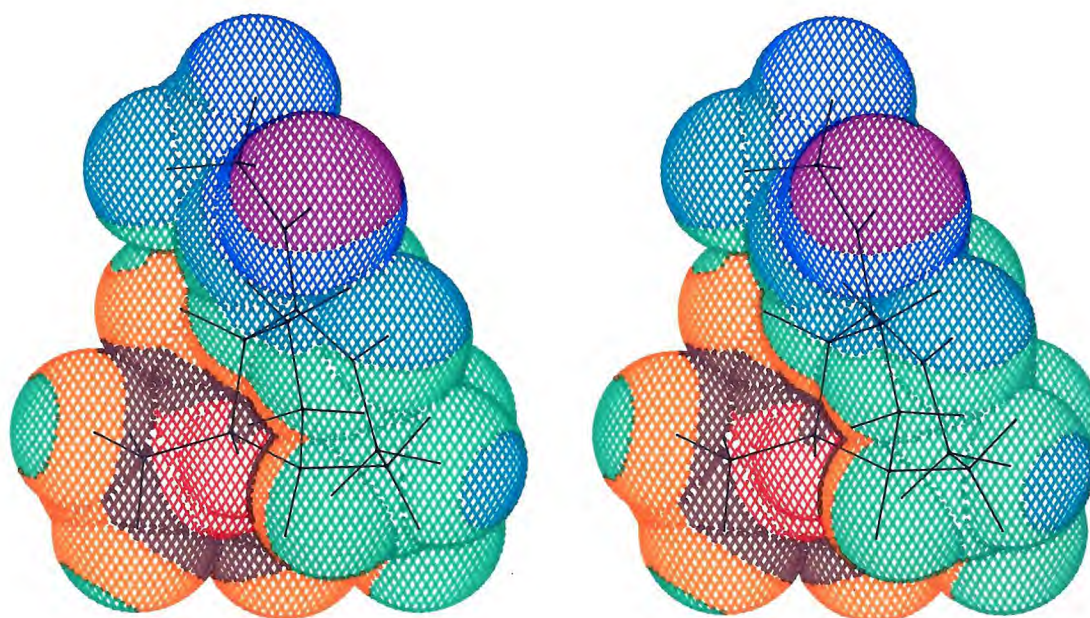


Figure 10. Color coded ESP on van der Waals surface of AlIAF.

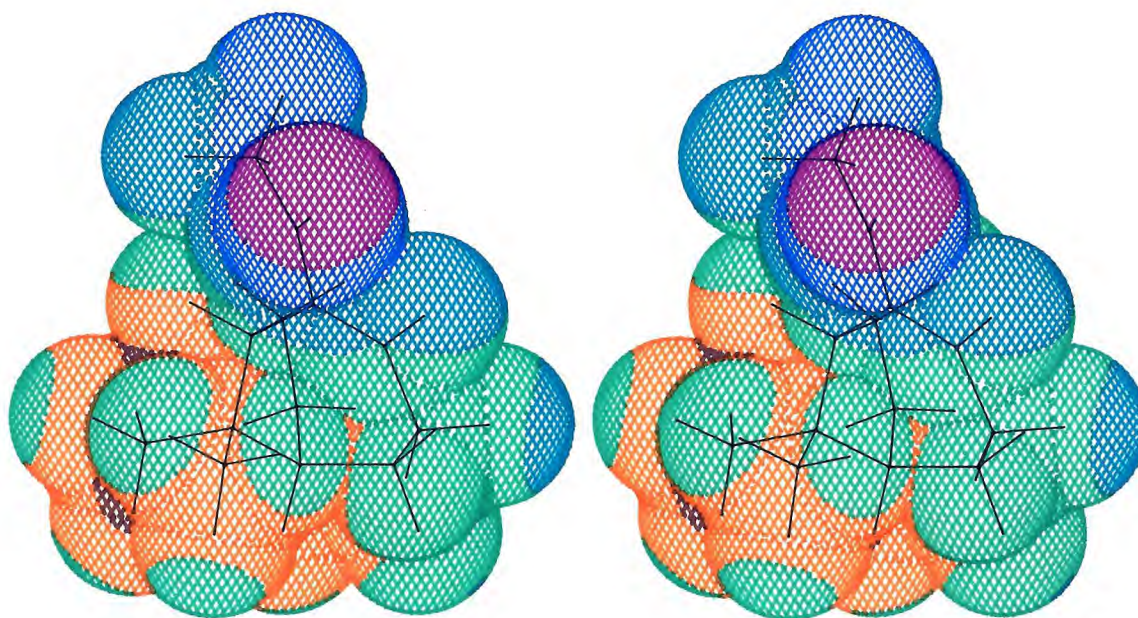


Figure 11. Color coded ESP on van der Waals surface of ANAN.

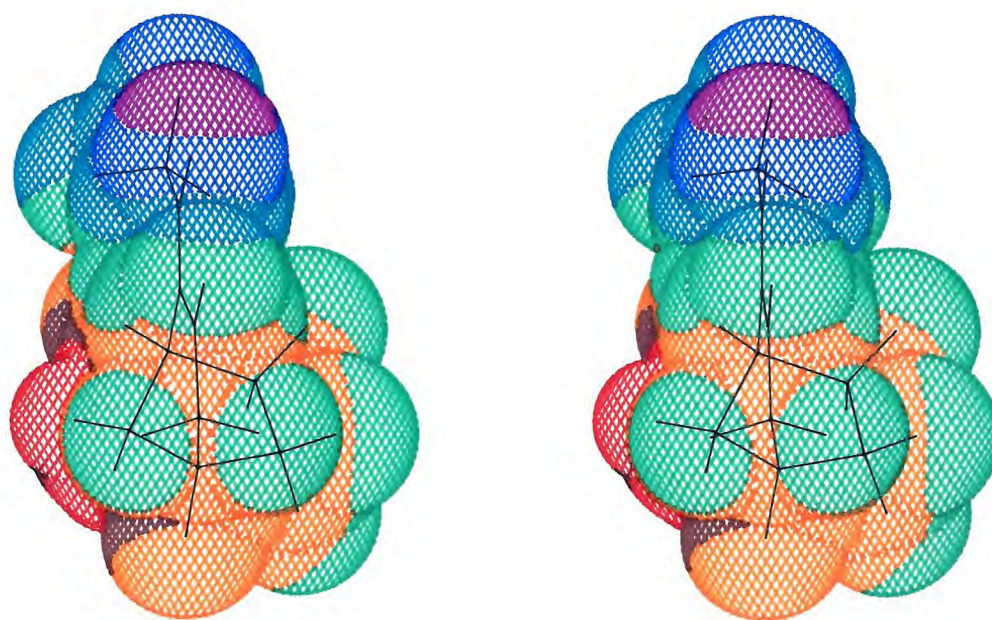


Figure 12. Color coded ESP on van der Waals surface of FERH.

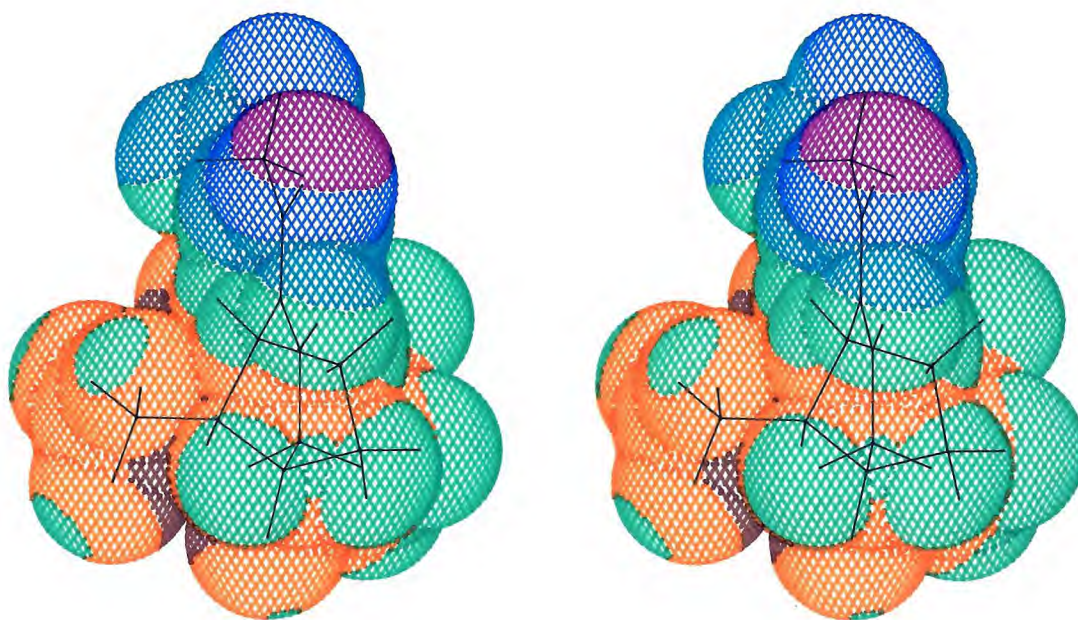


Figure 13. Color coded ESP on van der Waals surface of FERC.

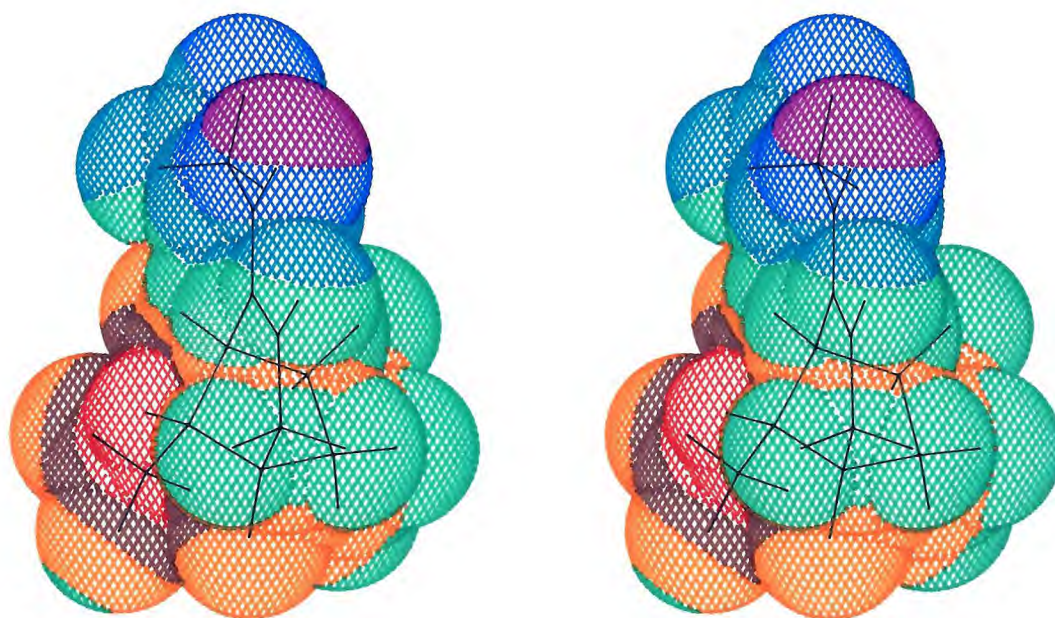


Figure 14. Color coded ESP on van der Waals surface of FERF.

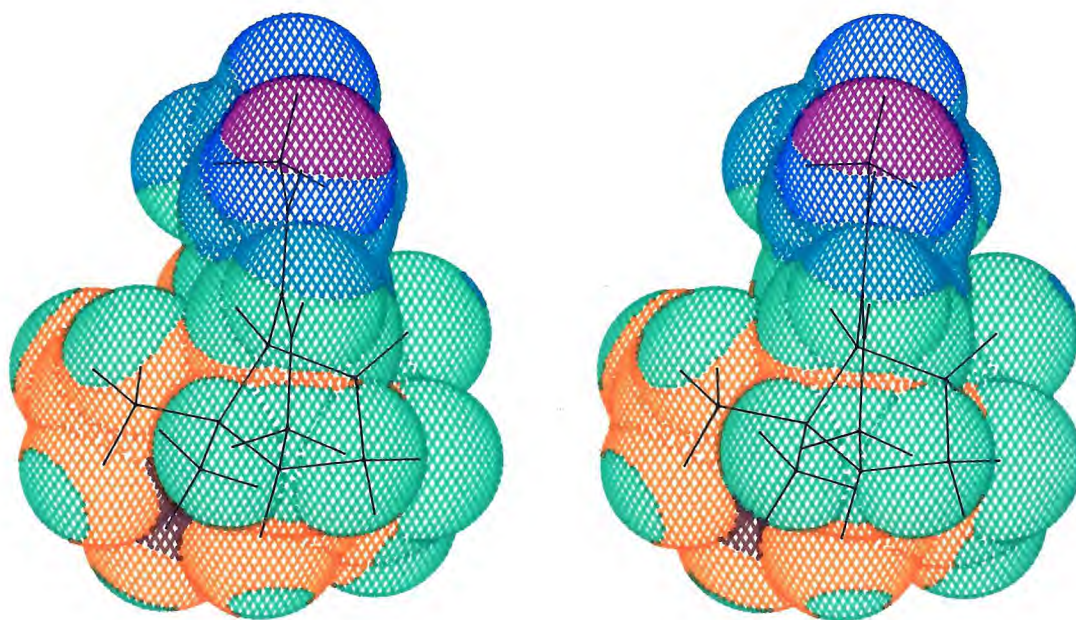


Figure 15. Color coded **ESP** on van der Waals surface of FERN.

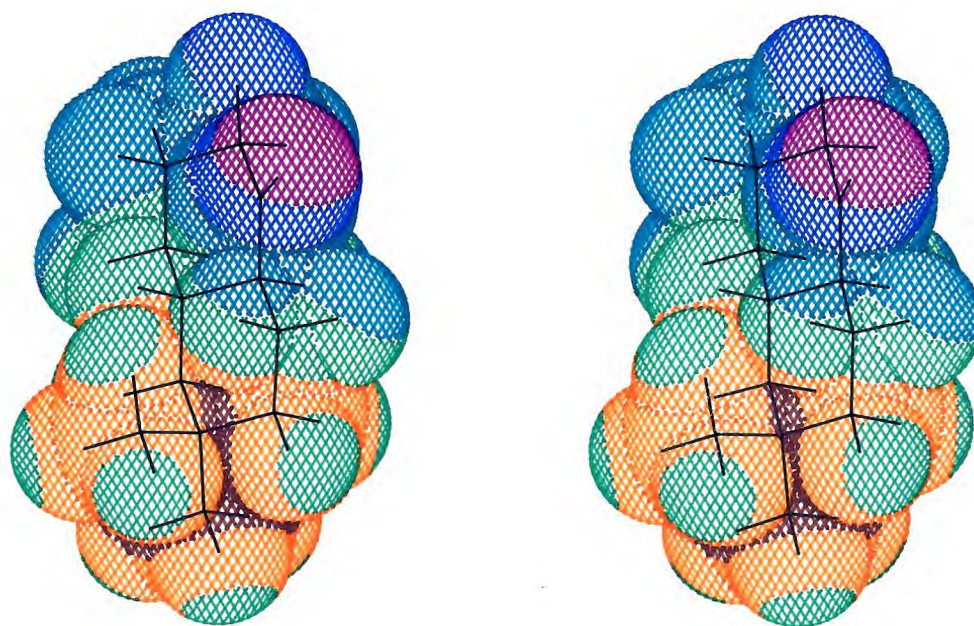


Figure 16. Color coded ESP on van der Waals surface of MET5Z.

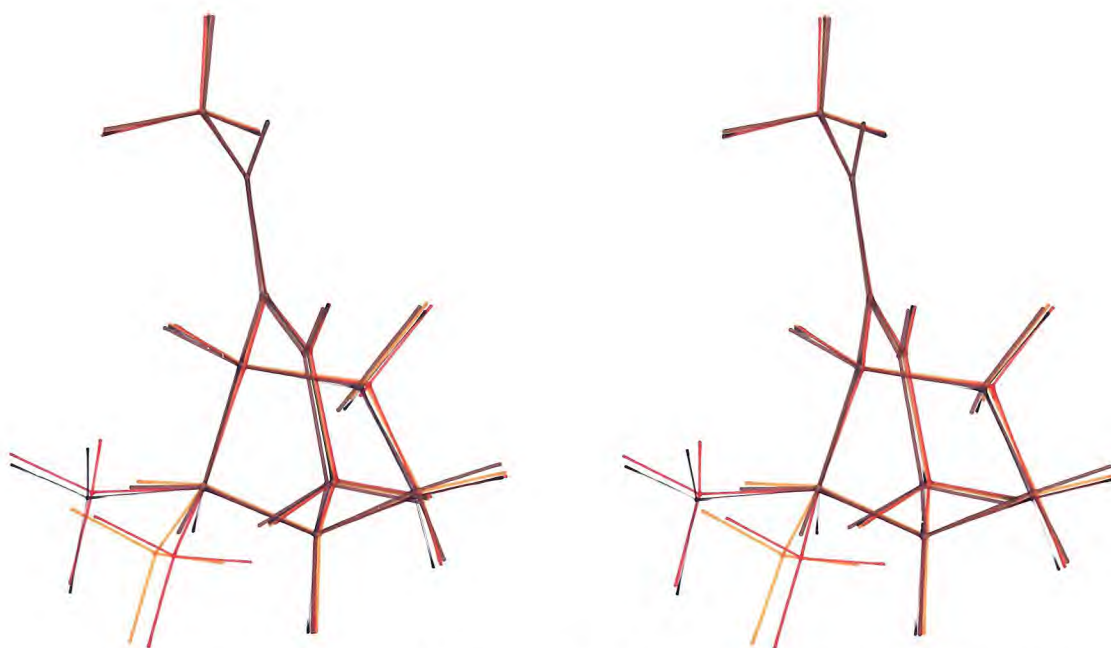


Figure 17a. Fitting on N C O in ferruginine series.
(isoarecolone-green, FERN-red, FERH-brown,
FERC-orange, FERF-black)

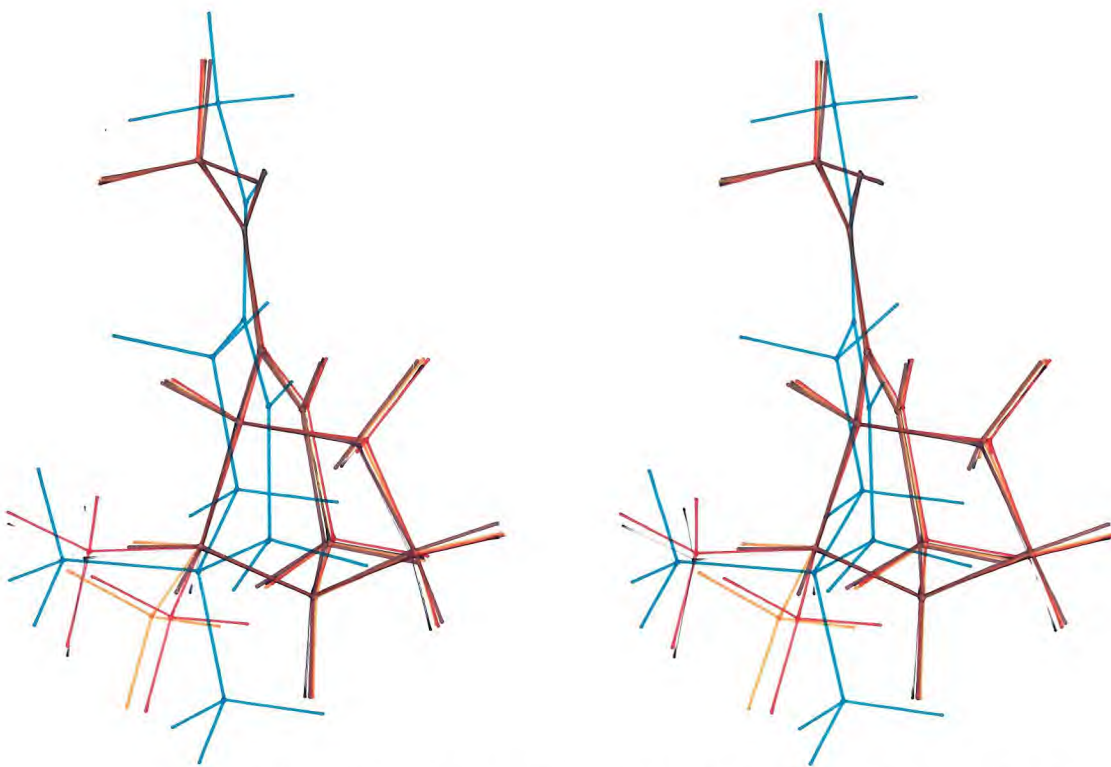


Figure 17b. Fitting on N C O of ferruginine series
with isoarecolone.

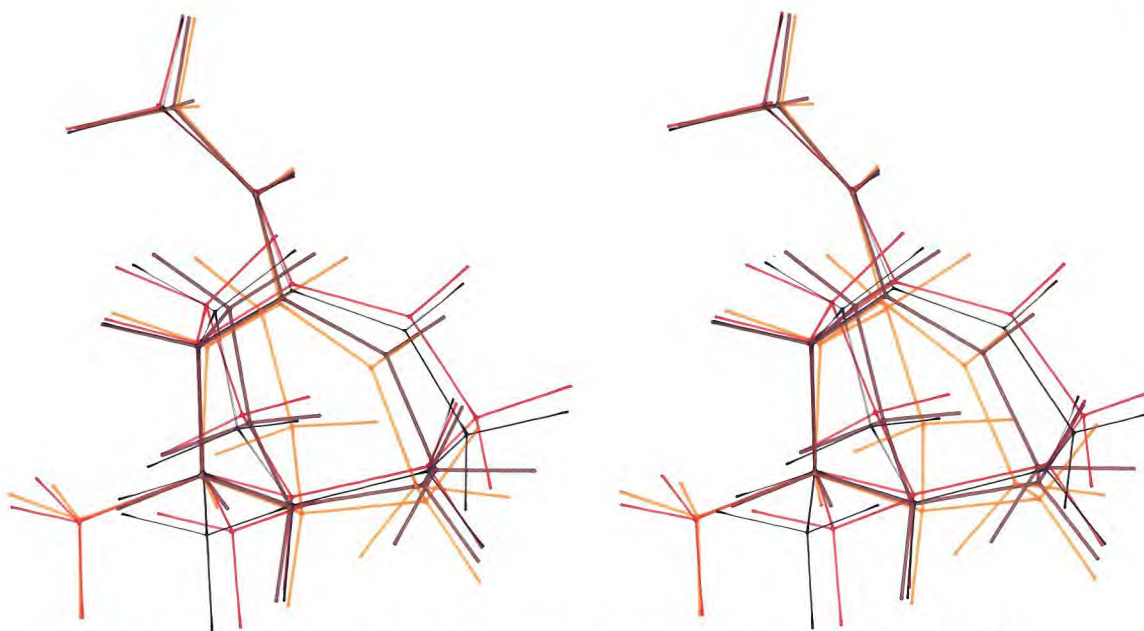


Figure 18a. Fitting on N C O in anatoxin series.
(isoarecolone-green, ANAN-red, ANAH-brown,
ANAC-black, ANAF-orange.) ,

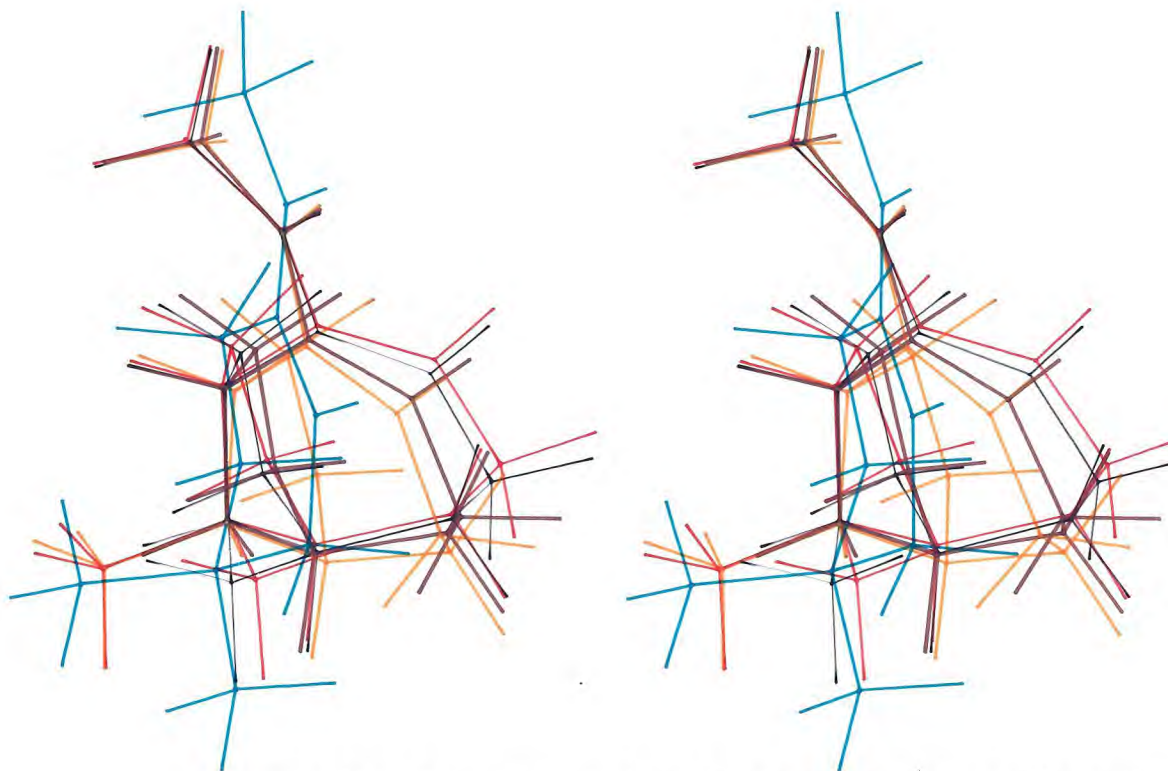


Figure 18b. Fitting on N C O of anatoxin series with
isoarecolone.

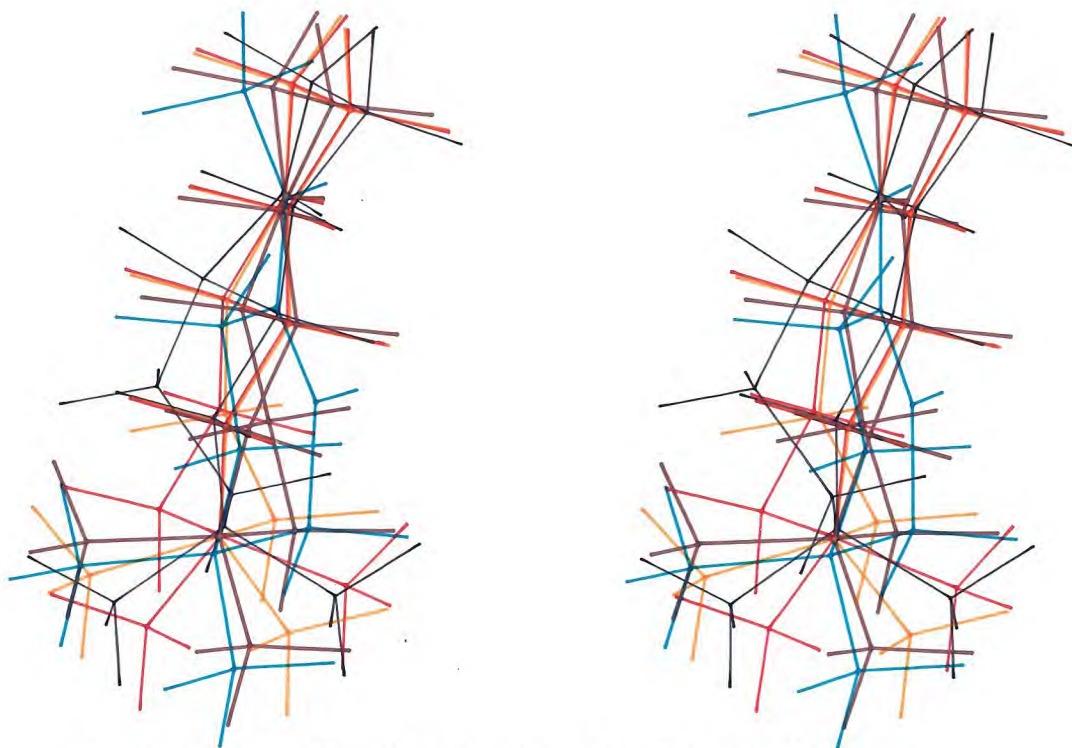


Figure 19a. Fitting on N C O of isoquinolone with isoarecolone.

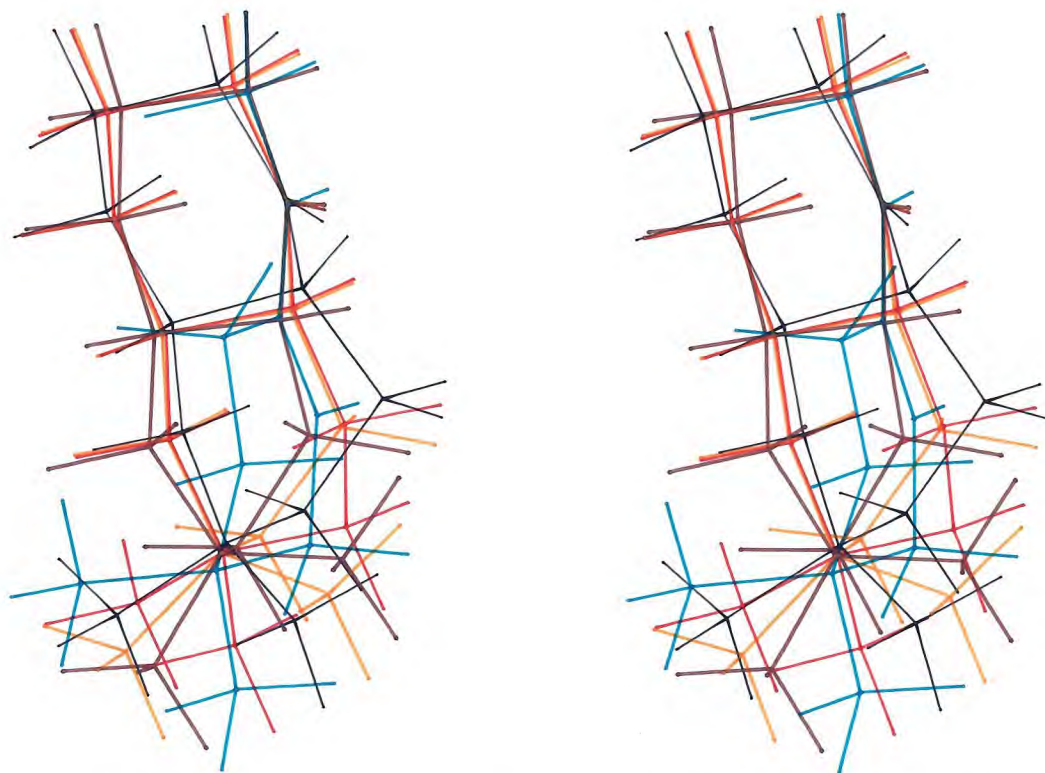


Figure 19b. Fitting on N C O of isoquinolone(Z) with isoarecolone.
(isoarecolone-green, MET1-purple, MET4-black, MET5-red, MET6-orange.)

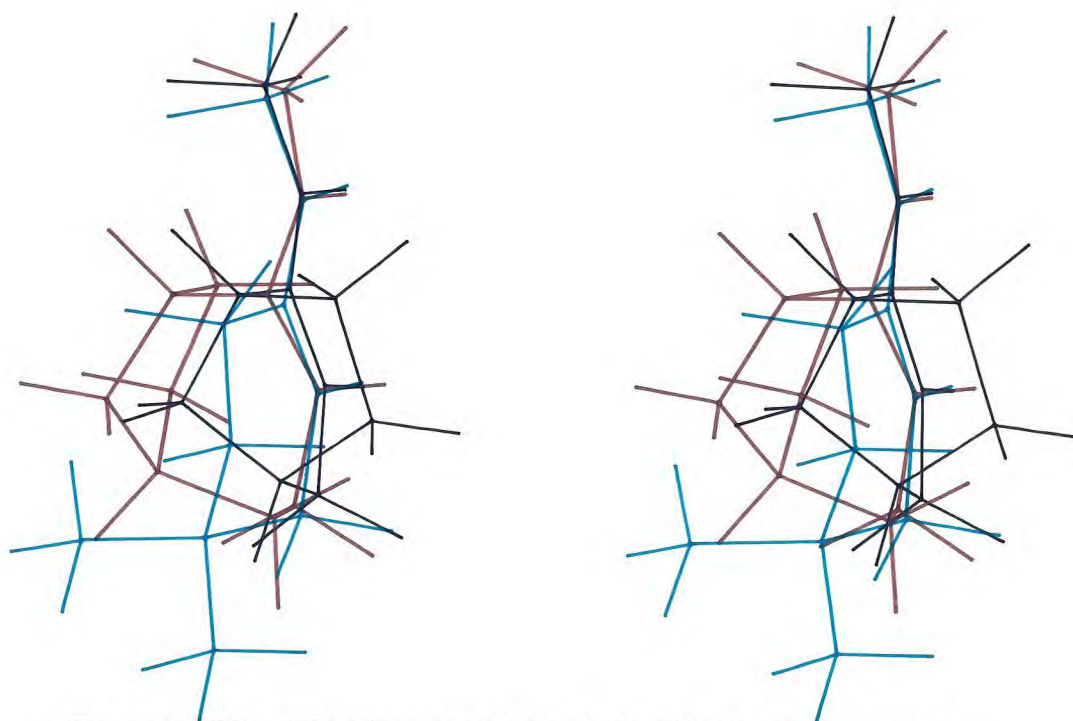


Figure 20. Fitting on $O=C-C=C$ of anatoxin and ferruginine with isoarecolone. (isoarecolone-green, anatoxin-black, ferruginine-brown)

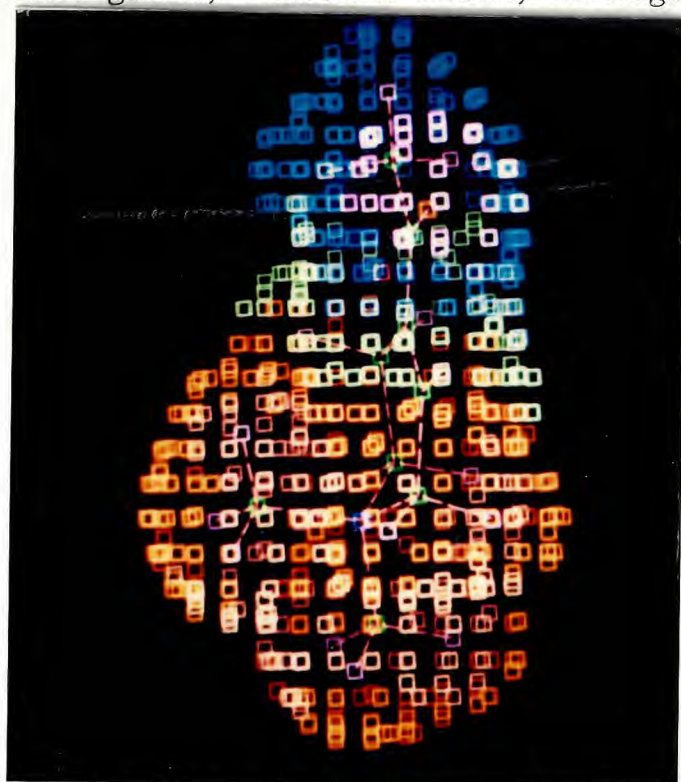


Figure 21. ESP using CAGECON method of isoarecolone.

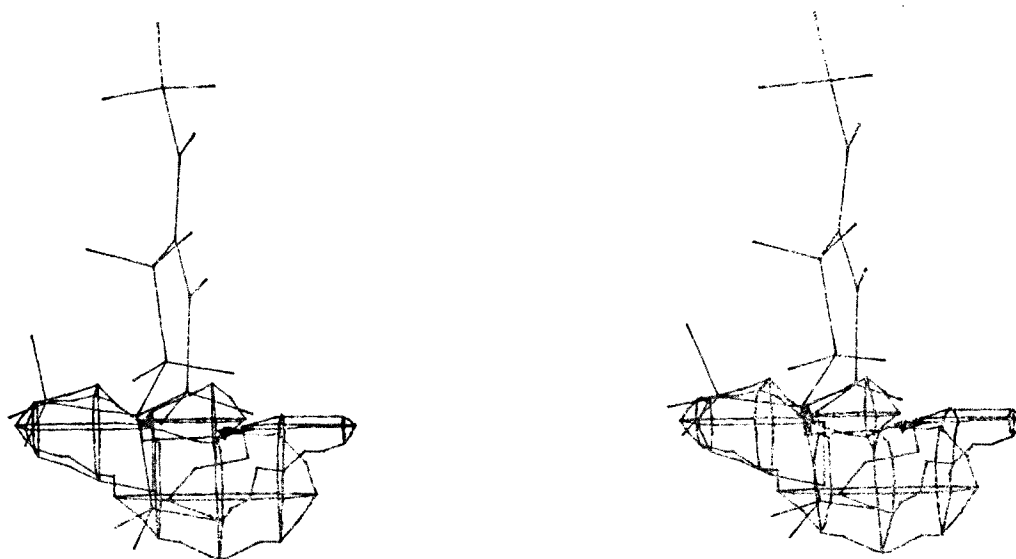


Figure 22. Contouring at 150 Kcal/mol of the ESP of isoarecolone

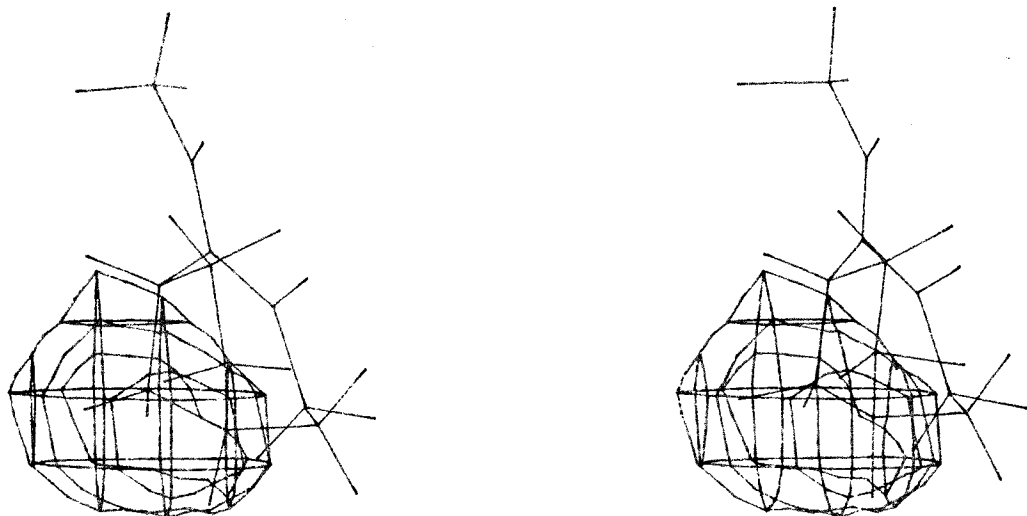


Figure 23. Contouring at 150 Kcal/mol of the ESP of ANAH

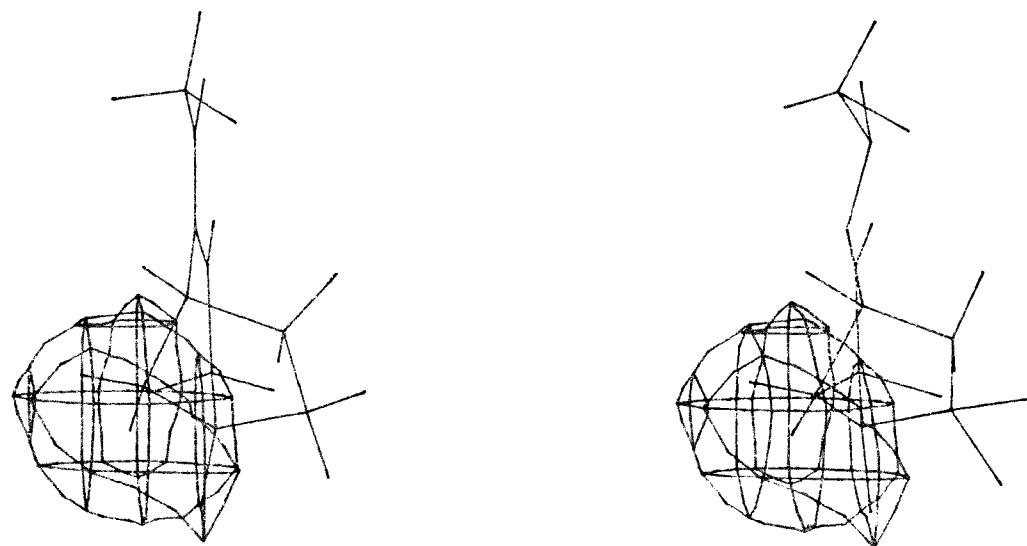


Figure 24. Contouring at 150 Kcal/mol of the ESP of FERH

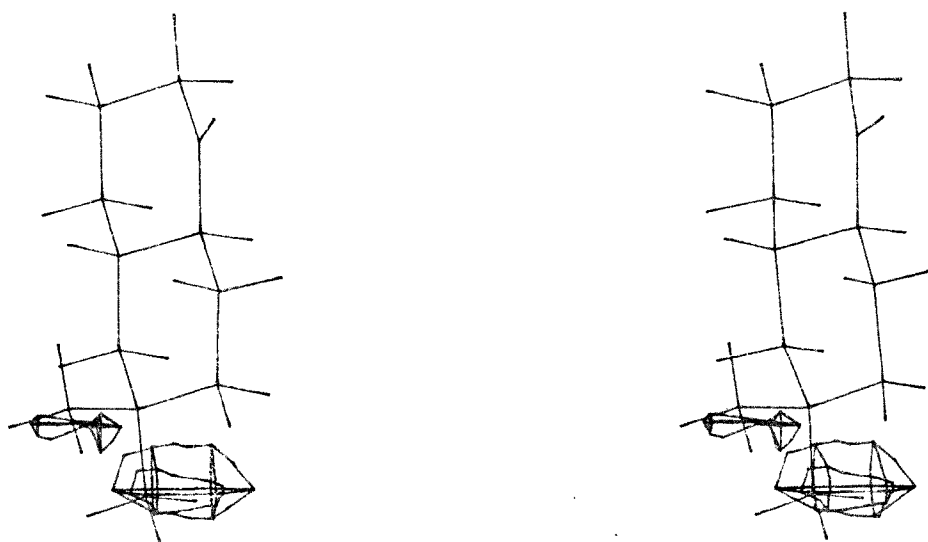


Figure 25. Contouring at 150Kcal/mol of the ESP of MET5Z

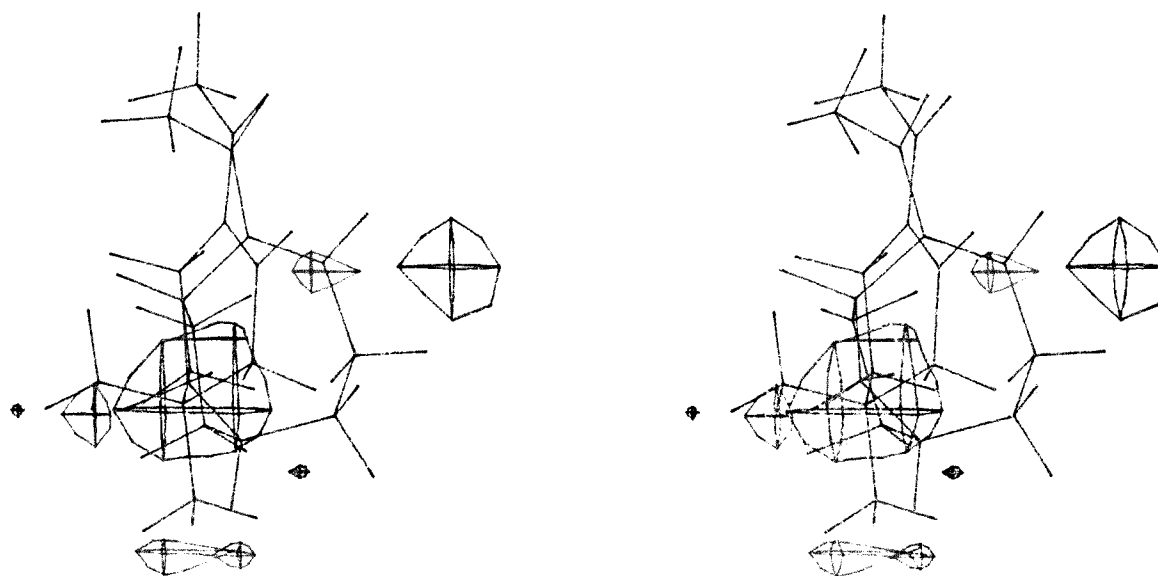


Figure 26. Contouring at 30Kcal/mol for the difference of ESP when anatoxin fit isoarecolone at N C O.

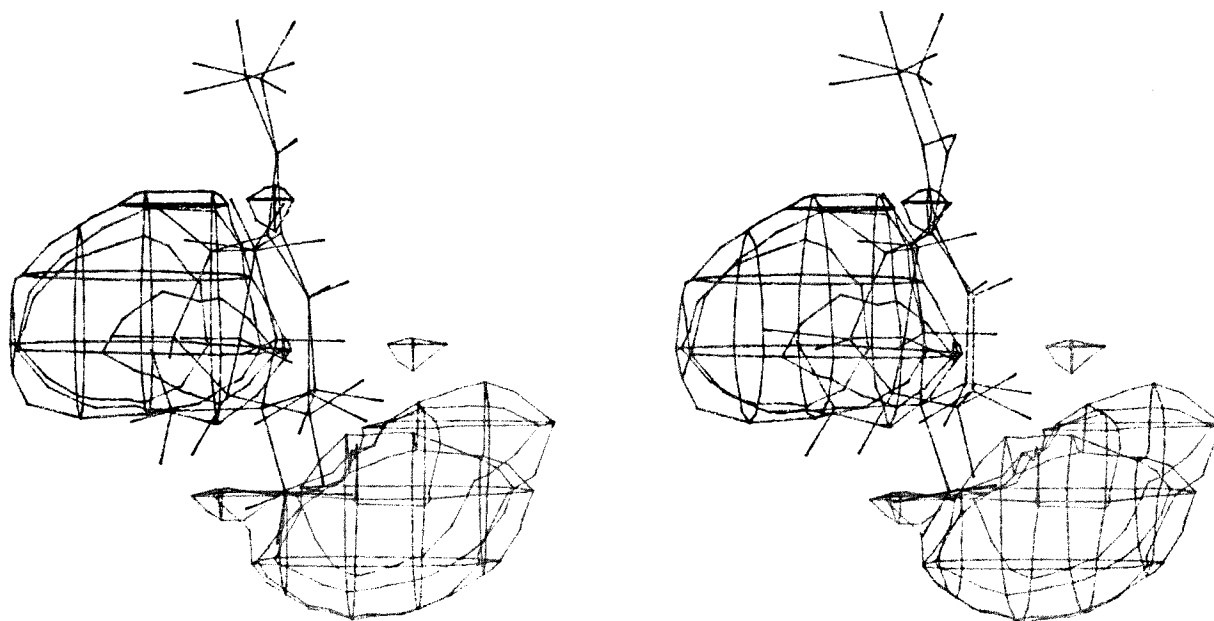


Figure 27. Contouring at 30Kcal/mole of the difference of ESP when anatoxin fit isoarecolone at C=C-C=C.

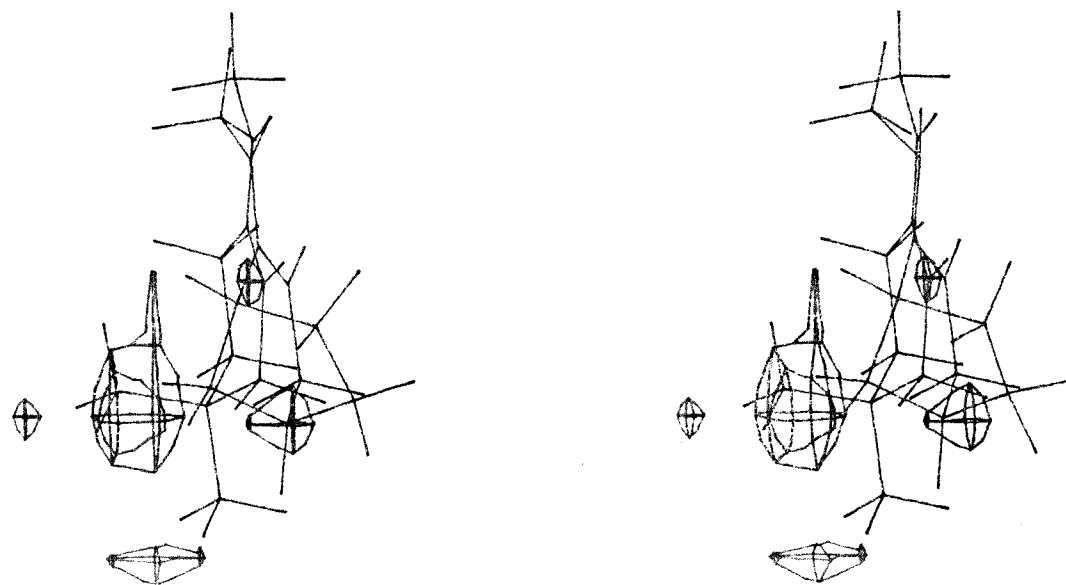


Figure 28. Contouring at 30Kcal/mol of the difference of ESP when ferruginine fit isoarecolone at N C O.

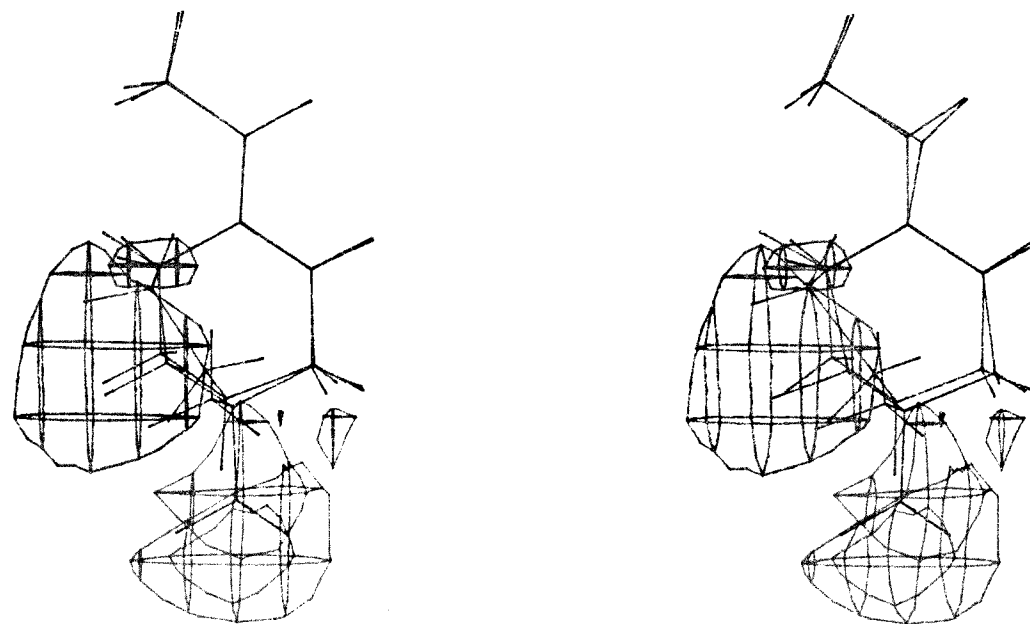


Figure 29. Contouring at 30Kcal/mol of the difference of ESP when ferruginine fit isoarecolone at C=C-C=C.

Appendix

PROGRAM SETS

```

C*****
C
C SETS implement sets operation in W.T.Wipke and T.M. Dyott, *
C J.Chem.Inf.Comput.Sci.,21,101(1981) *
C *
C Written for VAX-FORTRAN by Shang, Wen-chung *
C Chemistry Department *
C New Jersey Institute of Technolohg *
C 323, Martin-luther Blvd. Newark *
C *
C*****

C Constant 32 is refer to bits per INTEGER*4 data type

C-----KAND take the logical AND of M and N -----

      FUNCTION KAND(M,N,I,J)
      INTEGER*4 M(200,4),N(200,4)
      KAND=0
      DO 10 IJ=1,4
10    IF (JIAND(M(I,IJ),N(J,IJ)).NE.0) KAND=1
      RETURN
      END

C-----ISM check if N is in set I -----

      FUNCTION ISM(I,N)
      INTEGER*4 I,N

      ISM=BJTEST(I,N-1)
      RETURN
      END

C-----KON check if NN is 1 in set I -----

      FUNCTION KON(I,NN)
      INTEGER*4 I(4)
      INTEGER INDEX,IREM
      LOGICAL ANS

```

```

N=NN-1
INDEX=N/32+1
IREM=JMOD(N,32)
ANS=BJTEST(I(INDEX),IREM)
I(INDEX)=JIBSET(I(INDEX),IREM)
KON=ANS
RETURN
END

```

C-----KOFF check if NN is 0 in set I -----

```

FUNCTION KOFF(I,NN)
INTEGER*4 I(4)
INTEGER    N
LOGICAL    ANS

N=NN-1
INDEX=N/32+1
IREM=JMOD(N,32)
ANS=BJTEST(I(INDEX),IREM)
I(INDEX)=JIBCLR(I(INDEX),IREM)
KOFF=.NOT.(ANS)
RETURN
END

```

C-----KNXM find the next 1 in I since L element -----

```

FUNCTION KNXM(I,L)
INTEGER*4 I(4)
INTEGER  N,M,J

IF (L.GT.128) THEN
  WRITE(*,*)'INDEX OUT OF RANGE'
  KNXM=0
  RETURN
ENDIF
N=L
INDEC=L/32+1
N=JMOD(L,32)
J=N
10 IF (BJTEST(I(INDEC),J)) GOTO 20
J=J+1
IF (J.GT.128) GOTO 30
INDEC=INDEC+(J/32)

```

```

      J=J-(32*INDEC)
      IF (INDEC.GE.5) THEN
        KNXM=0
        RETURN
      ENDIF
      GOTO 10
20  KNXM=J+1+(INDEC-1)*32
30  IF (KNXM.GT.128) KNXM=0
      RETURN
      END

```

C-----ZEROM fill A array with 0-----

```

      SUBROUTINE ZEROM(A,N)
      INTEGER*4 A(N)

      DO 10 I=1, N
10  A(I)=0
      RETURN
      END

```

C-----ICNT check how may 1 are in I set -----

```

      FUNCTION ICNT(I,MAX)
      INTEGER*4 I

      ICNT=0
      DO 10 J=0,MAX-1
      IF (BJTEST(I,J)) ICNT=ICNT+1
10  CONTINUE
      RETURN
      END

```

C-----KSUB take the difference of IS1 and IS2 -----

```

      FUNCTION KSUB(IS1,IS2)
      INTEGER*4 IS1(4),IS2(4)
      INTEGER*4 I,J
      LOGICAL ANS

      ANS=.TRUE.
      I=0
10  J=KNXM(IS1,I)
      IF (J.EQ.0) GOTO 20

```

```
IF (KKOFF(IS2,J)) THEN
  ANS=.FALSE.
  GOTO 20
ENDIF
I=J
GOTO 10
20 KSUB=ANS
RETURN
END
```


PROGRAM CAGECON

```

C*****
C CAGECON read the CSS file from CHEMX and calculate ESP of *
C the dummy atom A then assign different color to it.      *
C                                                           *
C Author: Shang, Wen-chung                                *
C New Jersey Institute of Technology                       *
C 323 Martin Luther Blvd. Newark                         *
C                                                           *
C*****
PROGRAM CAGE
PARAMETER (NUTA=3000,NATY=60)
CHARACTER*2 JTYPEE,JTYPEN,ELTYP, DUMC
CHARACTER*50 ID
CHARACTER*80 ID1, ID2, ID4
CHARACTER*1 ACH
COMMON /TITL/ ID1, ID2, ID, ID4
COMMON /ATOM/ X(NUTA,3),CHARG(NUTA),ITYPE(NUTA),PRAD(NUTA)
COMMON /ATON/ JTYPEE(NUTA), JTYPEN(NUTA), NAT(NUTA),ICN(NUTA,4)
DIMENSION QLV(8)
IU=1
CALL READDAT(IU,NS,N)

C
C FOR003.DAT should contain the contour levels
C
READ(3,*)NLV
DO 50 J=1, NLV
50 READ(3, *) QLV(J)
CLOSE(UNIT=3)
DO 100 I=NS+1, N
IF ( JTYPEE(I).NE.' A') GOTO 100
CALL POTENT(X(I,1), X(I,2), X(I,3), NS, POT)
IF (POT.LT.QLV(1)) JTYPEN(I)='1 '
DO 80 J=2, NLV-1
IF (POT.GT.QLV(J).AND.POT.LT.QLV(J+1))JTYPEN(I)=CHAR(J+48)//' '
80 CONTINUE
IF (POT.GT.QLV(NLV)) JTYPEN(I)=CHAR(NLV+48)//' '
100 CONTINUE
CALL WRITEDAT(2,N)
END

SUBROUTINE POTENT(TPX,TPY,TPZ,N,POT)

```

```

C           CALCULATES POTENTIAL ENERGY (POT) OF AN ELECTRON
C           AT POINT (TP) IN A FIELD OF (N) CHARGES WITH
C           COORDINATES (X) AND CHARGE (CHAR).
C           DIELECTRIC CONSTANT EQUALS ONE.

```

```

C           POT= 332.1 * SUM(CHARG(I)/DIST(I))

```

```

PARAMETER (NUTA=3000)
COMMON /ATOM/ X(NUTA,3),CHARG(NUTA),ITYPE(NUTA),PRAD(NUTA)
COMMON /ATON/ JTYPEE(NUTA), JTYPEN(NUTA), NAT(NUTA),ICN(NUTA,4)

```

```

POT=0.0
DO 100 I=1,N
  DX=TPX-X(I,1)
  DY=TPY-X(I,2)
  DZ=TPZ-X(I,3)
  DXYZ=DX*DX+DY*DY+DZ*DZ
  DXYZ=SQRT(DXYZ)
  POT=POT+CHARG(I)/DXYZ

```

```

100 CONTINUE
POT=POT*332.1
RETURN
END

```

```

C.....READ DAT FILE.....

```

```

SUBROUTINE READDAT(IU, NS, N)
PARAMETER (NUTA=3000,NATY=60)
CHARACTER*2 JTYPEE,JTYPEN,ELTYP
CHARACTER*50 ID
CHARACTER*80 ID1, ID2, ID4
COMMON /TITL/ ID1, ID2, ID, ID4
COMMON /ATOM/ X(NUTA,3),CHARG(NUTA),ITYPE(NUTA),PRAD(NUTA)
COMMON /ATON/ JTYPEE(NUTA), JTYPEN(NUTA), NAT(NUTA),ICN(NUTA,4)
NS=0
READ(IU,9105)ID1
READ(IU,9105)ID2
READ(IU,9101) N,ID
READ(IU,9105)ID4
DO 200 I=1,N
READ(IU,9102) NAT(I),JTYPEE(I),JTYPEN(I),(X(I,J),J=1,3),
*           (ICN(I,J),J=1,4),CHARG(I)
IF ( JTYPEE(I).NE.' A' ) NS=NS+1

```

```

200  CONTINUE
9101  FORMAT(I4,7X,A50)
9105  FORMAT(A80)
9102  FORMAT(I4,A2,A2,2X,3F10.5,1X,4I4,16X,F8.3)

```

```

RETURN
END

```

```

C----- WRITE CSS FILE -----

```

```

C

```

```

SUBROUTINE WRITEDAT(IU, N)
PARAMETER (NUTA=3000,NATY=60)
CHARACTER*2 JTYPEE,JTYPEN,ELTYP
CHARACTER*50 ID
CHARACTER*80 ID1, ID2, ID4
COMMON /TITL/ ID1, ID2, ID, ID4
COMMON /ATOM/ X(NUTA,3),CHARG(NUTA),ITYPE(NUTA),PRAD(NUTA)
COMMON /ATON/ JTYPEE(NUTA), JTYPEN(NUTA), NAT(NUTA),ICN(NUTA,4)
WRITE(IU,9103)ID1
WRITE(IU,9103)ID2
WRITE(IU,9101) N,ID
WRITE(IU,9103)ID4
DO 200 I=1,N
WRITE(IU,9102) NAT(I),JTYPEE(I),JTYPEN(I),(X(I,J),J=1,3),
*           (ICN(I,J),J=1,4),0,0,0,0,CHARG(I)

```

```

200  CONTINUE
9101  FORMAT(I4,7X,A50)
9102  FORMAT(I4,A2,A2,2X,3F10.5,1X,8I4,F8.3)
9103  FORMAT(A80)
RETURN
END

```

Sample contour level file

```

7
0
40
60
80
100
120
140

```

CHEM-X ATOM COLORING COMMAND

```
*SET ATOM  
/COLO A1 PURPLE  
/COLO A2 BLUE  
/COLO A3 LBLUE  
/COLO A4 GREEN  
/COLO A5 ORANGE  
/COLO A6 BROWN  
/COLO A7 RED  
/COLO A8 LGREEN  
/FINISH
```

Reference

- [1] a) Review: G. Lunt and R. Harrison, *Biochem. Soc. Trans.* **8**, 693–694 **1980**:
b) Review: S.M. Aquilonius, *Parkinson's disease, Curr. Progr. Probl. mang. Porc. No. Eur. Symp. 1979*, U.K. Rinne, M. Klinger, G. Stamm, Ed., Elsevier, Amsterdam, **1980**, 17–27; c) M.C. Gerald, *Pharmacology, an Introduction to Drugs* and Ed. Prentice Hall Inc., Englewood Cliffs, N.J., **1981**, p. 128–147, L.A. Kepner and O.L. Wolthuis, *eur. J. Pharmacol.*, **48**, 377–382 **1978**
- [2] L.B. Kier, *Mole. Pharmacol.*, **3**, 487 **1967**
- [3] K.W. Reed, W.J. Murray, E.B. Roche and L.N. DonelSmith, *Gen. Pharmac.*, **12**, 177–185 **1981**
- [4] Beers and Reich, *Nature*, **228**, 917 **1970**
- [5] P. Pauling in *The conformation of Anticholinergic substances*, J.C. Stoclet, Ed., *Adv. Pharmacol., Ther., Proc. 7th Int. cong. Pharmacol.*, pergamon, **1979**, p. 302, P. Pauling and N. Datta, *Anticholinergic Substances: a single consistent conformation*, *Proc. Nat. Acad. Sci. U.S.A.* **77**, 708–712 **1980**. P. Pauling and T.F. Petcher, *Chem. Comm.* 1001–1002 **1969**
- [6] H. Weinstein, R. Osman, W.D. Edwards and J.P. Green, *Int. J. Quantum Chem., Quantum Biol., Symp.* **5**, 229 **1978**.
- [7] C. Humblet and G.R. Marshall, *Drug Devel. Res.*, **1**, 409 **1981** P. Gund, *Progr. Mol. and Subcell. Biol.*, **5**, 177 **1977**; P. Gund, *Ann. Repts. Med. Chem.*, **14**, 299 **1979**
- [8] B. Pullman, P. Courriere and J.P. Coubeils *Mol. Pharmacol.* **7**, 297–405 **1971**

- [9] Reynolds, Palmer *Acta Cryst. B22*, 1431–1439 **1970**.
- [10] A. T. Balaban, T. S. Balaban *J. Comp. Chem.*, **1985** *6*, 316–329
- [11] W. T. Wipke, T. M. Dyott *J. Chem. Info. Comput. Sci.*, **1975** *15*, 140.
- [12] K. Paton: *Commun. Assoc. Comput. Mach.*, **1969** *12* 514.
- [13] B. L. Roos-kozel and W. L. Jorgensen, *J. Chem. Inf. Comput. Sci.*, **1981**,*21*, 140 .
- [14] E. J. Corey and G. A. Peterson, *J. Am. Chem. Soc.*, *94*, 460
- [15] J. B. Hendrickson, D. L. Grier, and A. G. Toczko *J. Chem. Inf. Comput. Sci.*, **1984** *24*, 195.
- [16] N. E. Gibbs: *J. Assoc. Comput. Mach.*, **12**, 514
- [17] L. Matyska, *J. Comput. Chem.*, **1988** *9*, No. 5, 455–459.
- [18] Spivak, C. E. ; Gund, T. M. ; Liang,R. F. ; Water,J. A. *Eur. J. Pharmacol.* **1986**, *120*, 127.
- [19] Review: Gund,T. M. ;Gund,P. H. *Molecular Structures and Energetics*,*4*; Liebman, J. F. , Greenberg,A.,Eds.; Verlag Chemie: Weinheim/Bergstr., Germany, **1986**; p 319.
- [20] (1) Burkert, U.; Allinger,N. L.*Molecular Mechanics*; ACS Monograph 177; American Chemical Society: Washington, DC, 1982; pp 1–319. (b) Allinger, N. L.; Yuh, Y. H. *Quantum Chemistry Program Exchange*, Prog. No.395 **1980**.
- [21] Program written by G. Smith, of Merck, Shape & Dohme, is available through Quantum Chemistry Program Exchange.

- [22] Snyder, J. Searle Pharmaceutical Co. , Chicago, Illinois, and Gund, T. M., New Jersey Institute of Technology: ammonium parameters will be submitted to Dr. Norman Allinger for incorporation into the MM2 program; otherwise parameters can be obtained by writing to the authors.
- [23] TRIPOS Associates, St. Louis, Mo. , 63117.
- [24] Chemical Design Ltd., Oxford, U. K.
- [25] Dewar, M. J. S. University of Texas, Houston, TX. MOPAC program available from the Quantum Chemistry Program Exchange.
- [26] ARCHEM: Hermsmeier, M; Gund, T. M. NJIT – unpublished.
- [27] Politzer, P. *Chemical Applications of Atomic and Molecular Electrostatic Potentials*, Politzer, P.; Truhbar. D.G.,Eds.; (Plenum Press: New York), **1981**.
- [28] Spivak, C. E.; Water, J.; Witkop, B.; Albuquerque, E. X. *Mol. Pharmacol.*, **1983**, *23*, 337.
- [29] Marshall, G. Washington University, St. Louis, MO, private communication.
- [30] Rex A Palmer, Jasmine H Tickle and Ian J Tickle, *J.Mol.Graphics* **1983** *1*, 94.
- [31] Jerome M. Schulman, Michael L. Sabio, Raymond L. Disch *Recognition of Cholinergic Agonists by the Muscarinic Receptor*. *J. Med. Chem.* **1983**, *26*, 817–823.
- [32] R. P. Sheridan, Ramaswamy Nilakantan, J. Scott Dixon, and R. Venkataraghavan. *J. Med. Chem.* **29**, 1986, 899–906
- [33] B. Pullman, PH. Courriere, and J. L. Coubeils. *Mol. Pharm.***7**, 397–405.